

**POLYHEDRON REPORT NUMBER 53****CHEMICAL VAPOUR DEPOSITION OF COPPER FROM  
(hfac)CuL COMPOUNDS****MARK J. HAMPDEN-SMITH\***

Department of Chemistry, University of New Mexico, Albuquerque, NM 87131, U.S.A.

and

**TOIVO T. KODAS\***Department of Chemical Engineering, University of New Mexico, Albuquerque, NM 87131,  
U.S.A.**CONTENTS**

1. INTRODUCTION . . . . .	699
2. STRATEGY FOR CHEMICAL VAPOUR DEPOSITION OF Cu . . . . .	700
3. CHEMICAL VAPOUR DEPOSITION . . . . .	704
4. SELECTIVE CHEMICAL VAPOUR DEPOSITION . . . . .	709
4.1. Interaction of ( $\beta$ -diketonate)Cu <sup>I</sup> L <sub>n</sub> compounds with SiO <sub>2</sub> surfaces . . . . .	711
4.2. Affect of added reagents during CVD of copper from (hfac)CuL compounds . . . . .	718
4.3. STM-defined copper patterns . . . . .	718
4.4. Selective deposition onto patterned Teflon substrates . . . . .	719
5. FORMATION OF PATTERNED FILMS BY ALTERNATIVE METHODS . . . . .	723
6. PRECURSOR DELIVERY AND METAL ALLOYS . . . . .	724
7. CONCLUSIONS AND FUTURE DIRECTIONS . . . . .	728

**1. INTRODUCTION**

Chemical vapour deposition (CVD) is a method of depositing films or coatings of a wide variety of materials by thermal reaction of metal-containing compounds.<sup>1-5</sup> Chemical vapour deposition of a material involves the transport of a volatile inorganic, metal-organic or organometallic molecule to a heated substrate where it can react to deposit a film of a desired material. Some of the steps in the CVD of any material, any of which may be rate-limiting, are identified in Fig. 1.<sup>6</sup> These steps involve transport of the precursor into the reactor and to the substrate (1), adsorption (2) and reaction (3) of the precursor, desorption of the supporting ligands or reaction byproducts (6) and their transport out of the reactor (7), further reaction of the remaining metal-organic fragment to form an atomic species (3) and then diffusion (4), nucleation and growth of the final material (5). For a particular system, the precursor feed rate into the reactor, precursor transport rate to the substrate, gas-phase reactions, surface reactions, adsorption/desorption of reactants, intermediates or products, or a combination of factors may be rate-determining, and the real situation is likely to be more complex than this simplistic representation. However, this simple picture represents a starting point to stimulate thought and the reader is referred to a recent book for details of the processes for various metals.<sup>1</sup>

\*Authors to whom correspondence should be addressed.

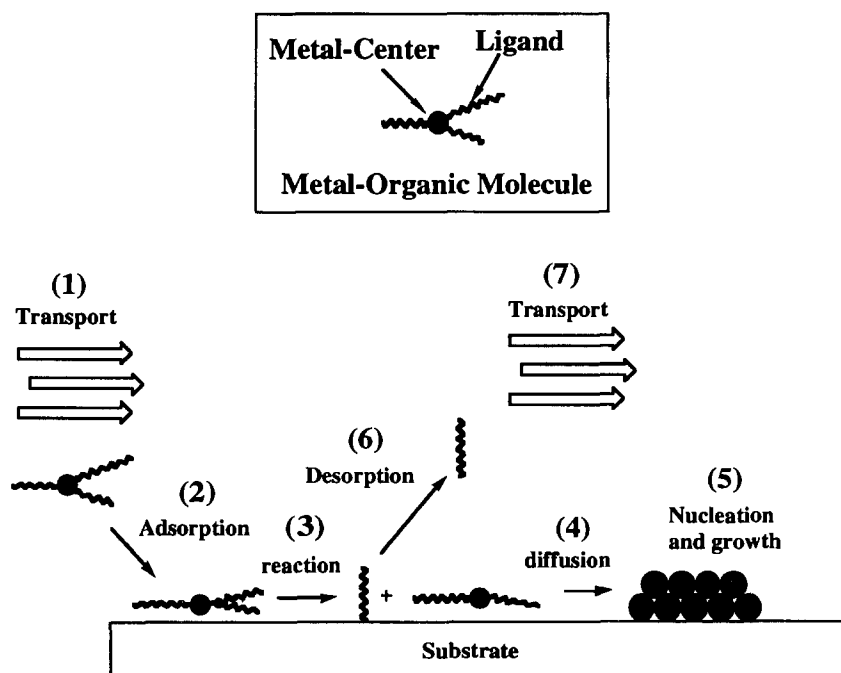


Fig. 1. Fundamental steps involved in CVD of an elemental material.

Some of the advantages of CVD over other (physical) deposition techniques, namely conformal coverage and selective deposition, are derived from the molecular nature of this process. Conformal coverage is the uniform coating of a complex topography substrate and results from the ability of the molecular precursor to penetrate complex surface features such as trenches by gas-phase diffusion. Selective deposition, the preferential deposition of a film on one substrate surface in the presence of another, can be achieved by a more rapid reaction on one surface compared to the other.

For insight into the processes involved in the CVD of molecular species in general, it is logical to set out to study a simple, model system. In principle, the CVD of an elemental material such as a metal should be a simple system which has all the attributes of CVD in general (some are identified in Fig. 1). It should also be possible to increase the complexity of the system by introducing other molecular precursors as sources of other elements to deposit binary or ternary materials such as alloys. In addition, there is significant technological interest in the CVD of certain metals for applications that vary from vertical interconnects in microelectronic devices<sup>3</sup> (W, Al, Cu) to permeable membranes for gas separations (Pd, Ag).<sup>7-9</sup> Copper is of interest for use in vertical interconnects in microelectronic devices as a result of its higher conductivity relative to tungsten and greater electromigration resistance compared to Al alloy used in existing interconnect schemes.<sup>10</sup>

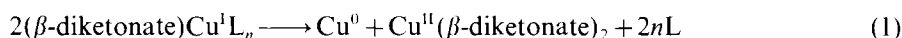
The goal of this Polyhedron Report is to describe our approach to the CVD deposition of copper which focuses on (i) design, synthesis and characterization of the molecular precursors, (ii) use of these precursors in CVD experiments under well-defined conditions, (iii) methods to obtain patterned films including etching and selective deposition of copper on metallic and polymer substrates in the presence of SiO<sub>2</sub> via surface modification and (iv) alternative methods for precursor delivery which allow use of precursors that are not compatible with traditional precursor delivery methods and also provide better control over stoichiometry for deposition of metal alloy films. In particular, we identify the strategy for this investigation and the pitfalls that were encountered during these studies.

## 2. STRATEGY FOR CVD OF Cu

A number of approaches are possible for the CVD of copper. In principle, copper(0) compounds would be the most desirable precursors because only ligand dissociation would be necessary to give the metal and should lead to the formation of high-purity films, as is the case for the CVD of Pt from Pt(PF<sub>3</sub>)<sub>4</sub>.<sup>11</sup> However, there are no examples of ligand stabilized copper(0) complexes in the

literature, and it seems that if it were possible to prepare them, they are unlikely to have sufficient thermal stability or volatility to be transported intact to a heated substrate. This leaves copper(I) and copper(II) compounds as possible candidates for the CVD of copper. Copper(II) compounds, particularly the  $\beta$ -diketonate derivatives, have now been used extensively for the CVD of copper films.<sup>10,12–23</sup> The derivative  $\text{Cu}(\text{hfac})_2$ , where  $\text{hfac} = 1,1,1,5,5,5$ -hexafluoroacetylacetonate deposits pure copper films only over the narrow temperature range of 340–380°C and at higher temperatures deposits highly contaminated films.<sup>24</sup> The addition of a reducing agent such as  $\text{H}_2$  solves this problem by lowering the deposition temperature to 250°C and this is an effective method for the CVD of Cu.<sup>18,25–28</sup>

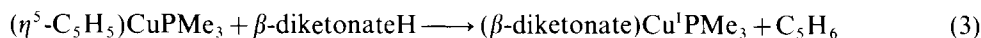
We chose to study the CVD of copper from a single reagent for simplicity and focused on the series of copper(I) compounds with the general empirical formula  $(\beta\text{-diketonate})\text{Cu}^{\text{I}}\text{L}_n$ . These species satisfy the design requirements of metal–organic precursors for CVD processes,<sup>6</sup> including sufficient volatility, especially where the  $\beta$ -diketonate ligands are fluorinated and they deposit high-purity copper films via thermally-induced disproportionation rather than thermal decomposition on a heated substrate according to the reaction of eq. (1).<sup>29–36</sup>



Thermally induced disproportionation has the advantage over thermal decomposition that it should be possible to avoid significant impurity incorporation in the growing copper film because it is not necessary for any of the ligands which support the copper(I) centre to be cleaved. Provided that disproportionation occurs at a lower temperature than thermal decomposition of either  $\text{Cu}^{\text{II}}(\beta\text{-diketonate})_2$  or L, the reaction of eq. (1) should be an efficient process to deposit high-purity copper films. This is indeed the case as we and a number of other research groups have discovered. Furthermore, these species allow investigation of the effect of systematic variation of the ligands, by changing the  $\beta$ -diketonate and L substituents, on the precursor properties and the properties of the copper films derived from CVD of these precursors. The ability to produce a very large number of precursors was an obstacle because many precursors were synthesized and characterized, only to be found unsuitable for CVD due to low volatility or thermal stability at typical delivery temperatures.

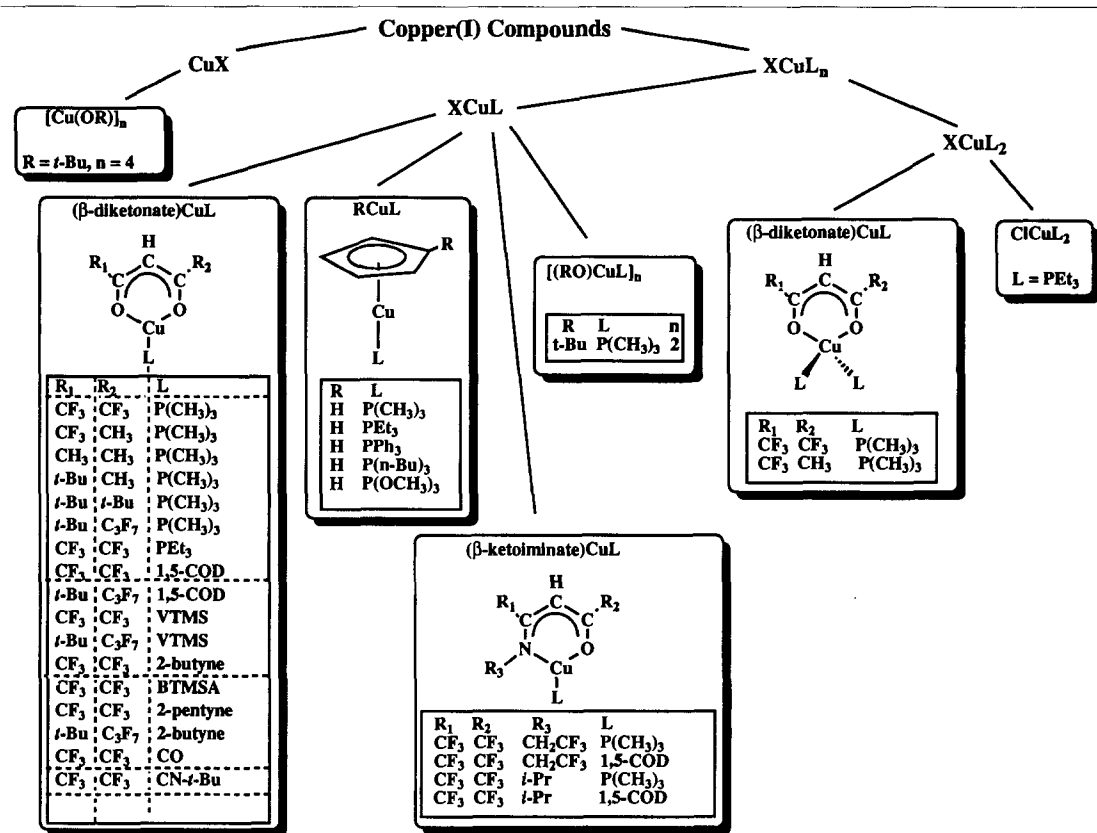
A number of species with empirical formula  $(\beta\text{-diketonate})\text{Cu}^{\text{I}}\text{L}_n$  have been described previously in the literature. The earliest report is that of Nast *et al.*<sup>37,38</sup> who described the synthesis of the ammonia adduct  $(\text{acac})\text{Cu}^{\text{I}}(\text{NH}_3)_{2.5}$  which is sufficiently thermally labile to undergo disproportionation at ambient temperature to form a copper mirror. There were other sparse examples of triorganophosphine and olefin adducts<sup>39–41</sup> until the more recent reports by us and other groups of this series of compounds motivated by the interest in their use as precursors for the CVD of copper.

The compounds  $(\beta\text{-diketonate})\text{Cu}^{\text{I}}\text{L}_n$  can be prepared by a variety of synthetic strategies including salt elimination, metallation and direct reaction with  $\text{Cu}_2\text{O}$ , each of which have different attributes.<sup>30,42–51</sup>



The compounds prepared by these methods are identified in Table 1, as a sub-set of the copper(I) precursors used for CVD of copper, and some representative examples of the solid-state structures of these compounds are presented in Fig. 2. Where possible, the direct reaction between  $\text{Cu}_2\text{O}$  and  $\text{hfacH}$  in the presence of L is simplest and produces a high yield of product that can be separated easily from the other by-product, water. In this reaction, the order of addition of the reagents is important to avoid formation of “ $(\beta\text{-diketonate})\text{Cu}$ ”, which disproportionates below  $-78^\circ\text{C}$ . It is therefore advisable to add an excess of the Lewis base reagent provided it can be separated from the reaction product in the next step. This is a critical problem because it has been shown that CVD rates and film properties from these compounds are very sensitive to the presence of additional reagents such as water,  $\text{hfacH}$  and L.<sup>25</sup> Furthermore, in some cases addition of an excess of the Lewis base can result in the formation of products that are not suitable for CVD of copper. For

Table 1. List of copper(I) compounds used for CVD of copper



example, the presence of two sterically demanding phosphine ligands such as (β-diketonate)Cu<sup>I</sup>(PCy<sub>3</sub>)<sub>2</sub> results in a severe distortion of the copper(I) coordination environment with significant lengthening of the Cu—O bond lengths (Fig. 3).<sup>42,52</sup> This leads to poor thermal stability, low volatility and makes the precursors unsuitable for CVD. Addition of an excess of PMe<sub>3</sub> in the reaction of eq. (2) results in the presence of four triorganophosphine ligands which gives complete displacement of the β-diketonate ligand from the copper(I) centre and the formation of an ionic salt such as [Cu(PMe<sub>3</sub>)<sub>4</sub>]<sup>+</sup> [hfac]<sup>-</sup>, as shown in Fig. 4. This species is involatile and is not useful for CVD.<sup>52</sup>

Analogous problems can result if insufficient amounts of Lewis bases are added during the reaction of eq. (2) if the Lewis base can potentially donate more than two electrons. This is the case for alkyne adducts where each π-bond can coordinate to a different copper(I) centre and has been demonstrated for the case of [(hfac)Cu]<sub>2</sub>(BTMSA), [(acac)Cu]<sub>2</sub>(BTMSA) and for comparison (hfac)Cu(BTMSA), as shown in Figs 5–7.<sup>53</sup>

Fluorinated Schiff base analogues of these β-diketonate compounds can also be prepared, see Figs 2 and 8, and display similar properties although they tend to be less suitable for CVD of copper films as a result of their lower volatility.<sup>54</sup> These species are of interest because they allow systematic changes in the characteristics of the uninegative ligand that cannot be made by changing the R group in the β-diketonate ligand.

The (β-diketonate)Cu<sup>I</sup>L<sub>n</sub> species have been characterized by a variety of spectroscopic and analytical methods. Some representative structural information has been presented in the figures above, and while this provides confirmation of the molecular formula and the degree of aggregation, it only provides information in the solid state which may not pertain to the structure and composition of these species in the gas phase. Molecular weight determinations in solution of representative examples of these compounds reveal that they are also monomeric in benzene solution, and it is likely that they are also monomeric in the gas phase. Evidence consistent with the low degree of

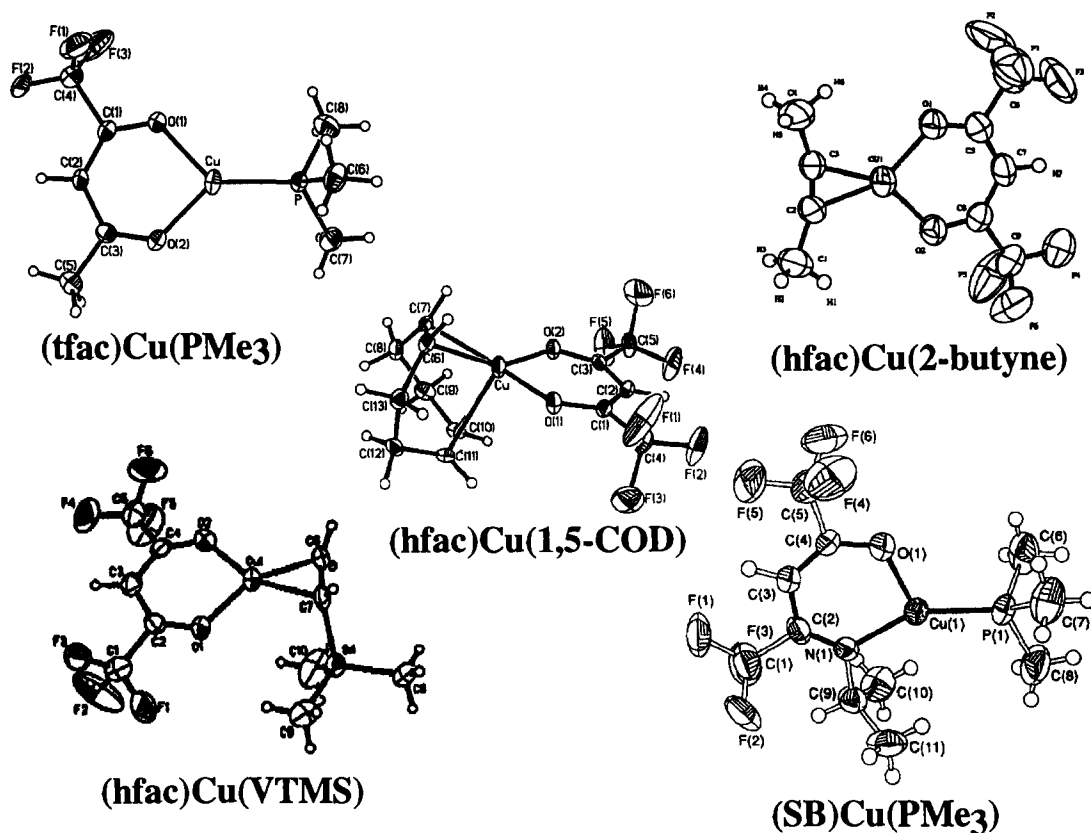


Fig. 2. Molecular structures of a number of ( $\beta$ -diketonate)Cu<sup>I</sup> L<sub>n</sub> compounds.

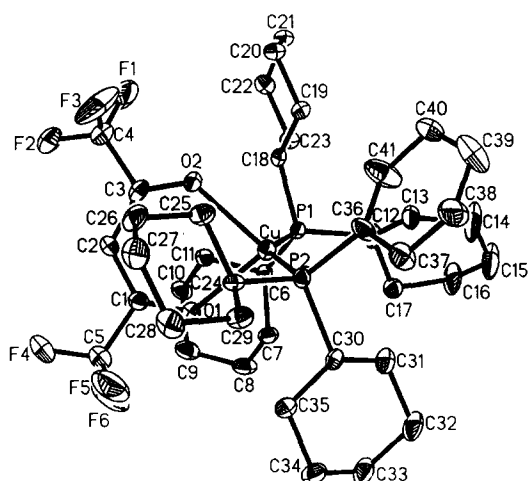


Fig. 3. Molecular structure of (hfac)Cu(PCy<sub>3</sub>)<sub>2</sub> (originally appeared in ref. 42).

molecular aggregation of these species is derived from measurements of their physical properties in the gas phase such as vapour pressure data. An example of some Clausius–Claypyron plots for (hfac)Cu(PMe<sub>3</sub>) and (hfac)Cu(1,5-COD) together with Cu(hfac)<sub>2</sub> for comparison are given in Fig. 9.<sup>34,43,55</sup> These data indicate that these (hfac)CuL species exhibit sufficient volatility for CVD. However, it is likely that the structure of some derivatives may be subtly different in the gas phase which may have profound effects on the adsorption behaviour of these species on different surfaces, as described later. An example of the possibility of structural changes between the solid-state and gas-phase structure is the case of (hfac)Cu(1,5-COD), where in the solid state the structure determined by single-crystal X-ray diffraction contained a copper(I) centre in a “3 + 1” coordination environment

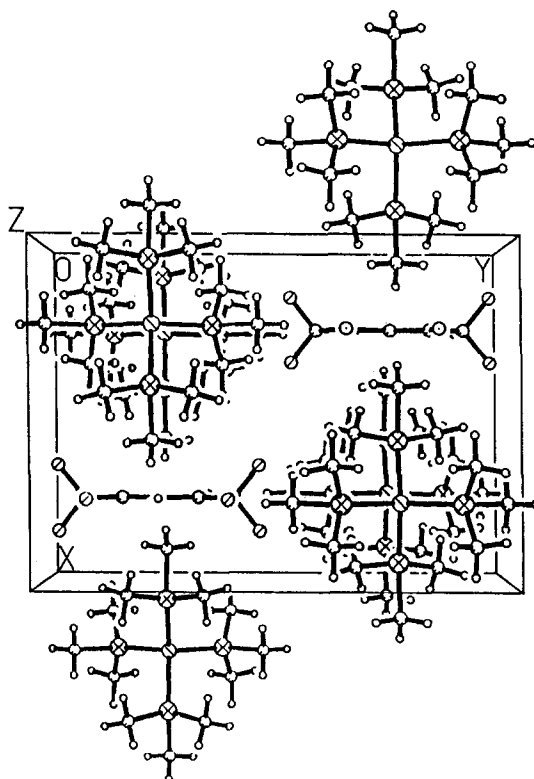


Fig. 4. Molecular structure of  $[\text{Cu}(\text{PMe}_3)_4]^+[\text{hfac}]^-$  (originally appeared in ref. 42).

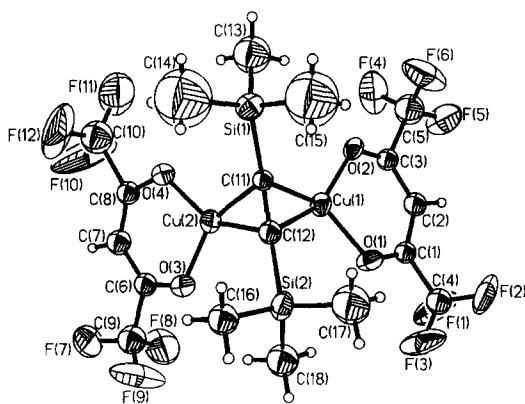


Fig. 5. Solid-state molecular structure of  $[(\text{hfac})\text{Cu}]_2(\text{BTMSA})$ .

as demonstrated in Fig. 2.<sup>44,50</sup> This structure is not retained on dissolution in non-coordinating solvents such as benzene as demonstrated by NMR spectroscopy,<sup>44</sup> and it is possible that the coordination environment of the copper(I) centre is quite different in the gas phase, as illustrated by the structure proposed in Fig. 10. As is the case for many CVD precursors, there is a distinct paucity of gas-phase structural information.

These observations illustrate the stringent requirement of volatility in precursors for CVD of materials which is often the hardest requirement to fulfill in metal-containing precursors.

### 3. CHEMICAL VAPOUR DEPOSITION

We have carried out chemical vapour deposition experiments in two different types of CVD reactors, each providing different information. Hot-wall CVD was conducted under conditions which ensured that there was complete conversion of the precursor to reaction products so that the

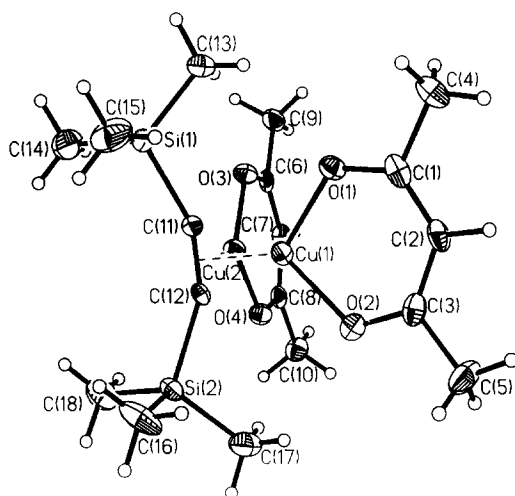


Fig. 6. Solid-state molecular structure of  $[(acac)Cu]_2(BTMSA)$ .

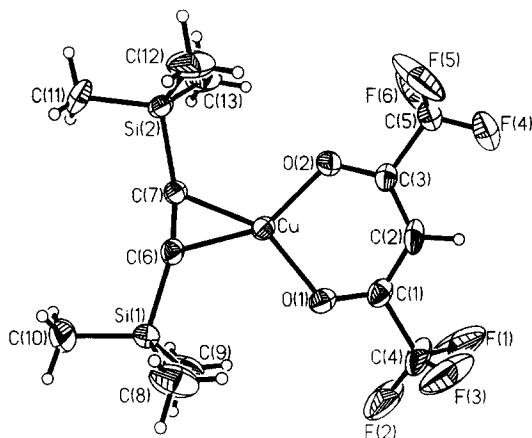


Fig. 7. Solid-state molecular structure of  $(hfac)Cu(BTMSA)$ .

overall reaction pathway could be quantified by mass balance. Warm-wall CVD using a lamp-heated substrate in a differential reactor, such as that shown in Fig. 11, was carried out under conditions where only a small portion of the precursor reacted such that the deposition rate was limited only by the rate of the surface reactions and not by the transport of the precursor into the reactor or to the substrate. In addition, the partial pressures of the reaction products remained low. This is a critical point because it allows the kinetics of the surface reaction to be observed under conditions where proposed surface reaction mechanisms are greatly simplified.<sup>56</sup>

Each reactor was operated at relatively low pressures, in the approximately 1–10 Torr regime, and in each case, the purity and properties of the deposited film were determined. Several difficulties were encountered in the early experiments. Deposition temperatures which were too high resulted in high-purity films but the resistivities were high because of the poor film morphology. Reactor pressures that were too low resulted in low deposition rates, poor reproducibility and poor film morphology. Substrate heating by contact with a hotter surface often resulted in selective CVD on the hotter surface and not on the substrate. Some compounds such as  $(hfac)CuPMe_3$ , which deposit selectively on metals in the presence of  $SiO_2$ , gave no deposition when  $SiO_2$  substrates were used, while other precursors which were less selective deposited on  $SiO_2$  substrates. These problems were in retrospect due to phenomena which can now be easily controlled but at the time caused major difficulties in carrying out and interpreting experiments.

These studies showed that the overall reaction pathway involved the disproportionation of the copper(I) compounds during steady-state growth of copper according to the reaction of eq. (1), and disproportionation occurred rapidly at relatively low temperatures (120–200°C).<sup>30–33,57</sup> Of all

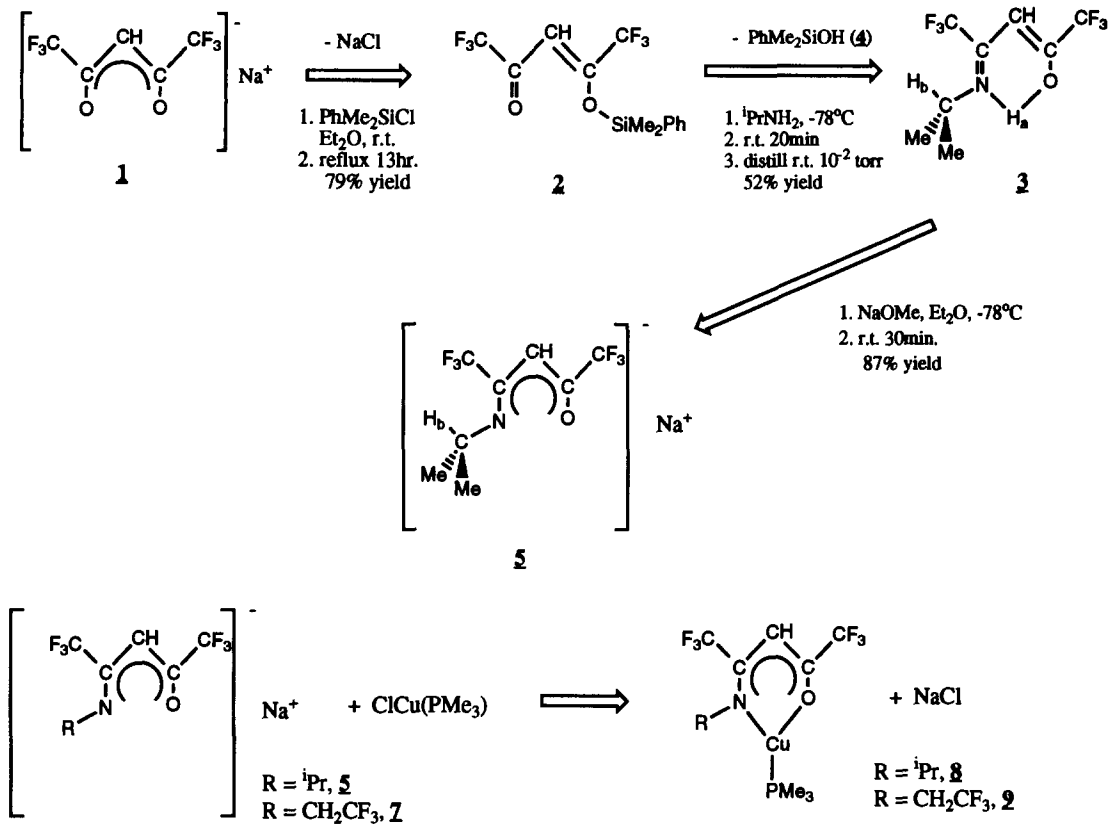


Fig. 8. Reaction scheme for the synthesis of fluorinated Schiff base copper(I) compounds (originally appeared in ref. 54)

### Vapor Pressure Data for (hfac)CuL Compounds

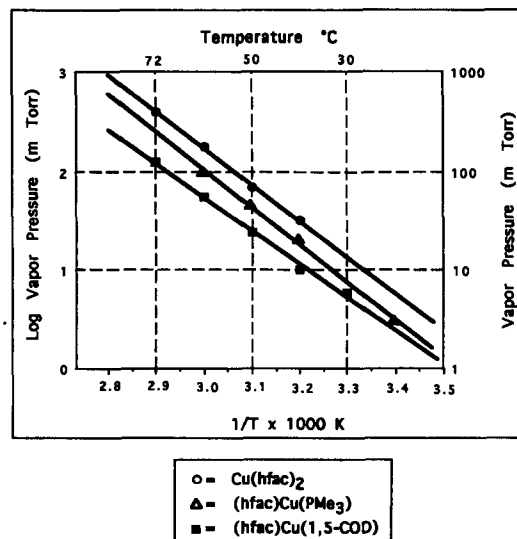


Fig. 9. Clausius-Claypryon plot for (hfac)Cu(1,5-COD), (hfac)Cu(PMe)<sub>3</sub> and Cu(hfac)<sub>2</sub>.



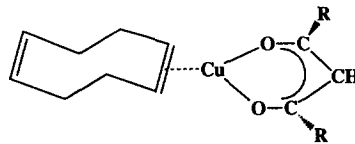


Fig. 10. Possible gas-phase structure of (hfac)Cu(1,5-COD).

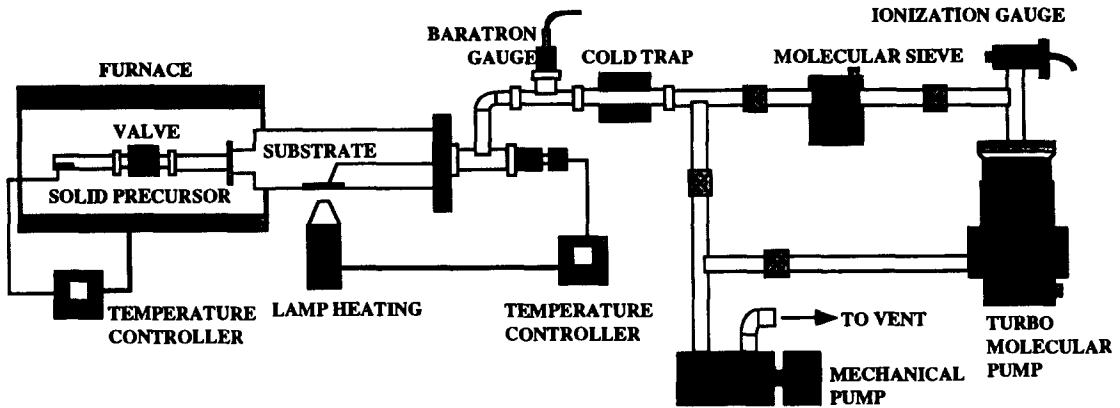
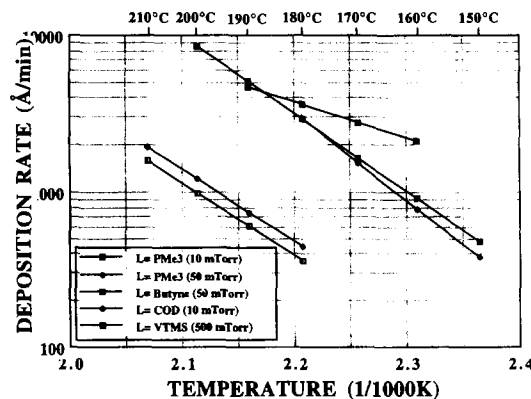


Fig. 11. Schematic drawing of the warm-wall reactor used for CVD of copper (originally appeared in ref. 33).

the derivatives in the series ( $\beta$ -diketonate) $\text{Cu}^{\text{I}}\text{L}_n$ , the species that are most suitable for the CVD of copper based on their volatility and thermal lability are (hfac)CuL where L = triorganophosphines such as  $\text{PMe}_3$  or  $\text{PET}_3$ , olefins such as 1,5-COD or VTMS (vinyltrimethylsilane) or alkynes such as 2-butyne.<sup>30-35,48,57</sup> The films deposited from these compounds have extremely high purity as determined by Auger electron spectroscopy (AES), X-ray photoelectron spectroscopy (XPS) and sputtered neutrals mass spectroscopy (SNMS) with resistivities close to bulk copper when the film morphology is good.

Deposition rates have been measured as a function of temperature for a number of compounds under surface-reaction-limited conditions and an Arrhenius plot is shown in Fig. 12.<sup>32-34,58</sup>

The plots of log deposition rate versus reciprocal temperature show that the deposition rate follows Arrhenius behaviour over the temperature range plotted. At higher temperatures the deposition rates are lower than that predicted by extrapolation of the Arrhenius plot consistent with a transition to transport- or feed-rate-limited deposition where the transport rate of the precursor to the substrate is not sufficiently high to keep up with the potential rate of the surface reaction. These plots reveal that for many of the compounds the activation energies are approximately  $25 \text{ kcal mol}^{-1}$ . Due to the rather limited range of precursor partial pressures that are available based on the equilibrium

Fig. 12. Plot of log deposition rate vs  $1/T$  for (hfac)CuL, where L =  $\text{PMe}_3$ , 1,5-COD and VTMS.

vapour pressures of this series of compounds, it has not been possible to measure the dependence of the deposition rate on the precursor partial pressure over a large pressure range, except for the case of (hfac)Cu(VTMS). As shown in Fig. 13, there is a significant difference in the activation energy at the two precursor partial pressures measured.<sup>59</sup>

The activation energies for CVD of copper from (hfac)Cu(VTMS) are 43(5) and 10(2) kcal mol<sup>-1</sup> at 10 and 500 mTorr precursor partial pressure, respectively. The precursor partial pressure variation of the deposition rate was also investigated over the partial pressure region 10–500 mTorr at a constant temperature of 160°C as shown in Fig. 14.<sup>59</sup> The deposition rate increased with increasing precursor partial pressure from 10 to 30 mTorr then became constant over the range 50–500 mTorr. Several assumptions, supported by data from separate experiments, were made in the interpretation

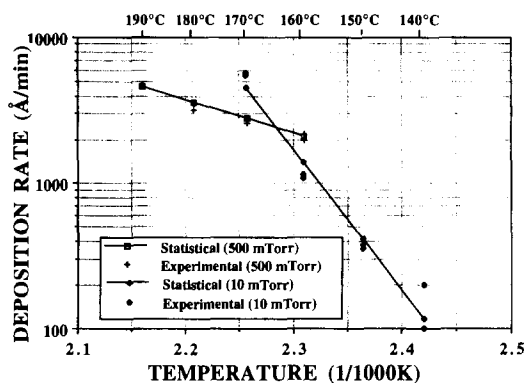


Fig. 13. Deposition rate of (hfac)Cu(VTMS) as a function of  $T^{-1}$  at constant precursor partial pressure of 10 and 500 mTorr.

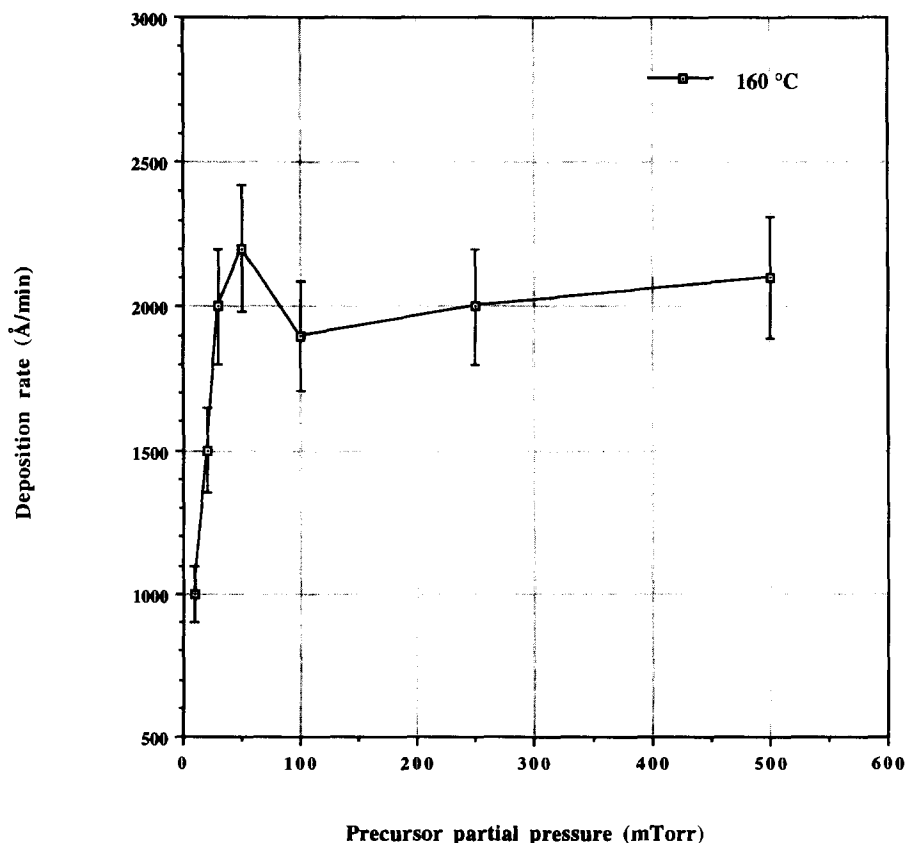


Fig. 14. Variation in deposition rate of copper from (hfac)Cu(VTMS) as a function of precursor partial pressure at constant temperature.

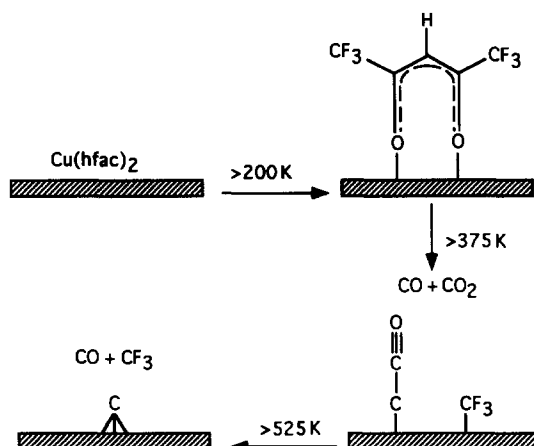


Fig. 15. Nature of the product of reaction of (hfac)Cu<sup>I</sup>L<sub>n</sub>, Cu(hfac)<sub>2</sub> or hfacH with Cu(100) surface as determined by reflectance FTIR.

of these results: (i) copper deposition occurs by disproportionation, (ii) ligand decomposition does not occur and (iii) the partial pressures of the reaction products were negligible. Based on these assumptions and the data available, mechanisms which involve dissociation of (hfac)CuL to (hfac)Cu and L were proposed to be rate-limiting. These rate expressions predict the observed precursor partial pressure dependence and that the activation energy at low pressures should be higher than that at higher pressures.

Other qualitative data that support this interpretation have been obtained by measurements of the adsorption behaviour of a variety of ( $\beta$ -diketonate)Cu<sup>I</sup>L<sub>n</sub>, Cu( $\beta$ -diketonate)<sub>2</sub>, L and  $\beta$ -diketone compounds on various surfaces under ultra-high vacuum (UHV) conditions. For example, treatment of Cu(100) with any of (hfac)Cu<sup>I</sup>L<sub>n</sub> results in cleavage of the Cu—L bond and formation of “(hfac)Cu”.<sup>17</sup> In addition, dosing the surface with Cu(hfac)<sub>2</sub> or hfacH results in the formation of a species which gives rise to an identical FTIR spectrum which is believed to have the structure shown in Fig. 15.

The surface chemistry of various copper(I) (and copper(II)) species has been studied under UHV conditions by a variety of surface science techniques. Under UHV conditions, direct observation of the bimolecular disproportionation reaction was not possible due to the low surface coverages. Instead, thermal decomposition of (hfac)CuL was observed (in the absence of a reducing agent such as H<sub>2</sub>). As a result, many of these studies, particularly of (hfac)CuL, where L = 2-butyne, 1,5-COD and VTMS on surfaces including Cu(100),<sup>17</sup> Cu(111),<sup>17</sup> Pt(111),<sup>60,61</sup> Ag<sup>34</sup> and TiN,<sup>62,63</sup> have focused on the thermal decomposition of these compounds. It was shown that (hfac)CuL underwent bimolecular disproportionation to form high-purity copper at pressures greater than 0.01 mTorr. In all these studies, the neutral ligand desorbs from the substrate surface intact. These observations were borne out by a separate temperature-programmed desorption (TPD) study of the neutral ligands 2-butyne, VTMS, 1,5-COD and PMe<sub>3</sub> from a Cu(100) surface which showed that these species desorbed intact at low temperatures (125, 175, 225 and 450 K, respectively), as shown in Fig. 16.<sup>17</sup>

The influence of the nature of the  $\beta$ -diketonate substituents on CVD of copper has only been studied qualitatively because the volatility and thermal stability of the precursors tend to decrease with decreasing fluorination of the substituents. The trends in minimum deposition temperature for CVD of copper from ( $\beta$ -diketonate)Cu(PMe<sub>3</sub>) are acac < tfac ~ fod<sup>51</sup> < hfac.<sup>31</sup> To date, hfac appears to be the most suitable  $\beta$ -diketonate ligand, and as a result, most studies have focused on (hfac)CuL compounds.

#### 4. SELECTIVE CHEMICAL VAPOUR DEPOSITION

Selective CVD refers to deposition of a material on one surface in the presence of another or on one area of a surface and not on another. There are a variety of methods by which selective deposition may be achieved, and these aspects have been reviewed recently.<sup>4,56</sup> In principle, the

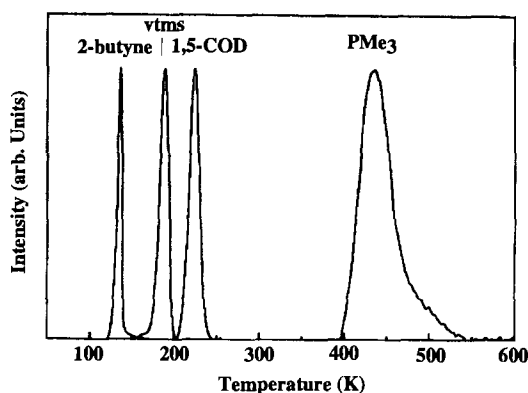


Fig. 16. TPD of neutral ligands from a Cu(100) surface (originally appeared in ref. 17).

problem can be reduced to consideration of the relative rates of the surface reaction and nucleation on the surface on which deposition is required (defined as the growth surface), and the surface on which deposition is to be avoided, often referred to as the non-growth surface, as illustrated in Fig. 17.

In order to achieve selective deposition, two strategies can be adopted: preferential enhancement of the rates of surface reaction and nucleation on the growth surface or preferential inhibition of the surface reaction and nucleation on the non-growth surface. The surfaces in question are clearly important since selective deposition is influenced by the nature of the reactive groups on the two surfaces. The technologically relevant substrates for the selective deposition of copper are likely to be diffusion barrier materials for the growth surface, which include Ta, W, TiN, W/Re alloy, TaSiN and dielectric materials such as SiO<sub>2</sub> or fluorinated polymers for the non-growth surface. Therefore, in order to promote the selective CVD of copper it is necessary either to enhance the deposition rate on a diffusion barrier or inhibit deposition on SiO<sub>2</sub> or a polymer.

In order to avoid any deposition at all on SiO<sub>2</sub> it is clear that the optimum strategy should at least involve a component that attempts to prevent deposition on SiO<sub>2</sub> completely. It may also be necessary to find a method to promote the reaction of the copper compounds on a diffusion barrier surface. As it happens, the compounds ( $\beta$ -diketonate)Cu<sup>I</sup>L<sub>n</sub> tend to disproportionate rapidly on conducting substrates such as W and, in many cases, on SiO<sub>2</sub>. The selective deposition of copper from ( $\beta$ -diketonate)Cu<sup>I</sup>L<sub>n</sub> compounds has been reported in a number of articles in the literature and these data are summarized in Table 2.

It is important to be careful when comparing the results of selective deposition from different research groups because the extent of selectivity will be strongly affected by the way in which each surface was prepared. For example, the functional groups present on a silica surface are very sensitive to the method of preparation and thermal history of the sample prior to the CVD experiment as is apparent from the discussion in the next section. In Table 2, the results of our studies are highlighted (italicized) because these experiments were carried out under identical conditions in the same reactors using substrates prepared under identical conditions. Therefore, this represents a true comparison of the inherent reactivity of the precursors on the different substrates. The overall conclusion from this comparison is that while (hfac)Cu(PMe<sub>3</sub>) selectively deposits copper on W and not SiO<sub>2</sub> over the temperature range 150–300°C, the compounds (hfac)CuL,

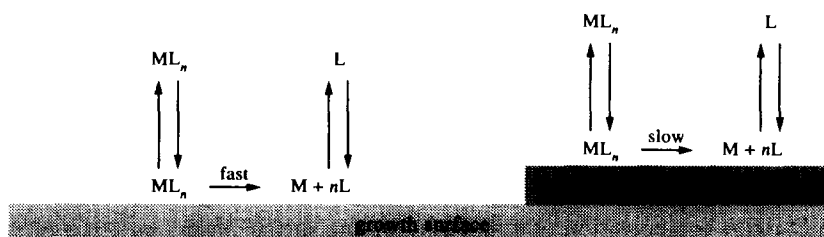


Fig. 17. Schematic diagram showing the principle of selective CVD on a growth surface vs a non-growth surface.

Table 2. Selective deposition of copper from ( $\beta$ -diketonate)Cu<sup>I</sup>L<sub>n</sub> compounds

Precursor	Selectivity	Temperature range	Reference
<b>a. (hfac)Cu(triorganophosphine)</b> (hfac)Cu(PMe <sub>3</sub> )	Pt, W, Cu vs SiO <sub>2</sub>	150–300 C	31, 57
<b>b. (hfac)Cu(olefin)</b> (hfac)Cu(1,5-COD)	none for Pt, W, Cu vs SiO <sub>2</sub>	120–250 C	31, 32
(hfac)Cu(1,5-COD)	certain degree of selectivity for Ta, Cu, Ag, Au and Cr vs SiO <sub>2</sub> and Si <sub>3</sub> N <sub>4</sub>	< 200 C	58
(hfac)Cu(VTMS)	none for W vs SiO <sub>2</sub>	120–250 C	59, 74, 75, 98
(hfac)Cu(VTMS)	none for TiN, TiSi <sub>2</sub> , Cu, Si vs SiO <sub>2</sub>	120–250 C	62
(hfac)Cu(VTMS)	W vs SiO <sub>2</sub>	120–420 C	35
	TiN vs SiO <sub>2</sub>	150–180 C	35
	PtSi vs SiO <sub>2</sub>	150–200 C	35
<b>c. (hfac)Cu(alkyne)</b> (hfac)Cu(2-butyne)	none for Pt, W, Cu vs SiO <sub>2</sub>	120–250 C	31, 33
(hfac)Cu(2-butyne)	Some selectivity for Co and Mo vs SiO <sub>2</sub>	120–250 C	48, 49

where L = 2-butyne, 1,5-COD and VTMS, deposit copper onto both W and SiO<sub>2</sub>. Therefore, it is logical to adopt a selective deposition strategy that prevents reaction of ( $\beta$ -diketonate)Cu<sup>I</sup>L<sub>n</sub> compounds with SiO<sub>2</sub> surfaces. To achieve this goal, it is necessary to understand the nature of the interaction of ( $\beta$ -diketonate)Cu<sup>I</sup>L<sub>n</sub> compounds with SiO<sub>2</sub> surfaces. This became the goal of this part of our research.

It is worth noting at this stage that the mechanisms of the interaction or reaction of ( $\beta$ -diketonate)Cu<sup>I</sup>L<sub>n</sub> compounds with a particular substrate are unlikely to be the same as that of steady-state growth on copper. It is likely that reaction occurs to form stable nuclei on which further reactions occur ultimately resulting in the formation of a continuous copper film. Therefore, the disproportionation mechanism does not necessarily occur for ( $\beta$ -diketonate)Cu<sup>I</sup>L<sub>n</sub> on a substrate surface.

#### 4.1. Interaction of ( $\beta$ -diketonate)Cu<sup>I</sup>L<sub>n</sub> compounds with SiO<sub>2</sub> surfaces

The interaction of various ( $\beta$ -diketonate)Cu<sup>I</sup>L<sub>n</sub> compounds with a model SiO<sub>2</sub> surface was studied in order to facilitate characterization.<sup>64–67</sup> The model SiO<sub>2</sub> surface chosen was Cab-O-Sil because it has a relatively high surface area, which enables the adsorption of a large amount of adsorbate per unit mass, and the nature of the surface functional groups has been well documented in the literature.<sup>68–70</sup> The same functional groups have also been observed on flat silica substrates such as those used in microelectronics applications.<sup>71</sup> The technique chosen to investigate the nature of adsorption of ( $\beta$ -diketonate)Cu<sup>I</sup>L<sub>n</sub> compounds on the silica surface was transmission FTIR. This technique is simple to implement, provides a sensitive indication of the nature of the surface functional groups and the adsorbate, and allows for rapid data collection. The adsorption experiments were carried out on the following copper(I) compounds, (hfac)CuL where L = PMe<sub>3</sub>, 2-butyne, VTMS, chosen because these represent a range of precursor selectivities for metals versus SiO<sub>2</sub> substrates (see below), and the species hfachL, where L = PMe<sub>3</sub>, 2-butyne and VTMS and the copper(II) compound Cu(hfac)<sub>2</sub>. The latter species are either known to be or likely to be reaction by-products liberated on silica surfaces. The experiments were carried out under a number of different conditions to allow study of the reaction or interaction between the adsorbate and the model silica surface. The silica surface was thermally pretreated to generate a range of surface

functional groups including hydrogen-bonded and isolated surface hydroxyl groups, strained four-membered siloxane rings and silica oxo groups. Three surfaces were prepared by dehydrating Cab-O-Sil powder under conditions of (i) evacuating at room temperature for 20 min under vacuum, which creates both hydrogen bonded and isolated surface hydroxyl groups, referred to as Surface III; (ii) heating Surface III to 400°C for 20 min, which creates a surface which possesses a higher ratio of isolated to hydrogen-bonded surface hydroxyl groups, referred to as Surface II; and (iii) Surface I, where Surface III has been heated to 850°C for 20 min, which results in complete dehydration of the hydrogen-bonded surface hydroxyl groups to form strained siloxane rings with retention of some isolated surface hydroxyl groups. The types of surface functional groups on these three surfaces are illustrated in Fig. 18.<sup>66</sup>

In a series of control experiments, the temperature dependent stretching frequencies of the surface functional groups over a temperature range -130 to +400°C was measured to ensure that subtle temperature-dependent changes in stretching frequencies were not misinterpreted. An example of the FTIR spectrum of Surface I is shown in Fig. 19. Each surface was dosed with the species named above at low temperatures (-130°C) and at room temperature (25°C) and the temperature dependent behaviour of the adsorbate was investigated on heating to 400°C. Although these

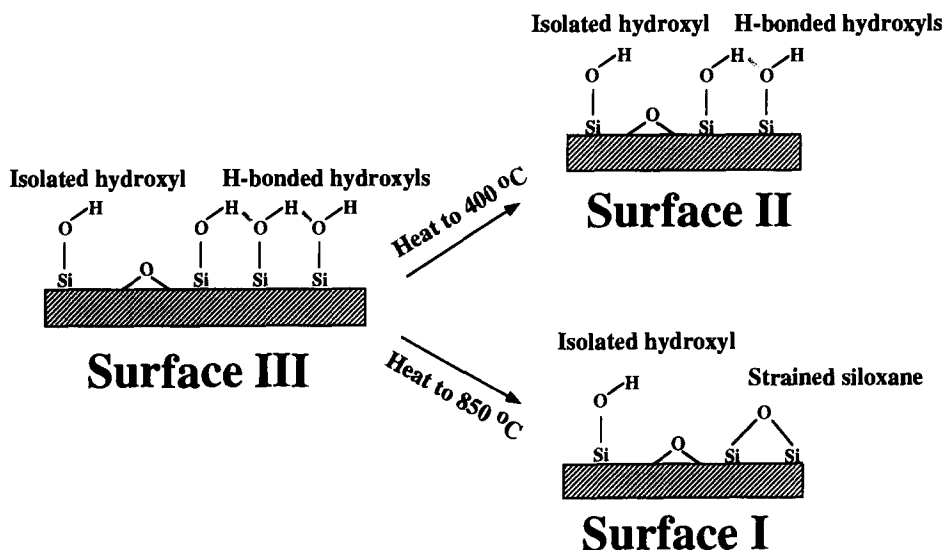


Fig. 18. Schematic representation of the surface functional groups on silica treated under different conditions (originally appeared in ref. 66).

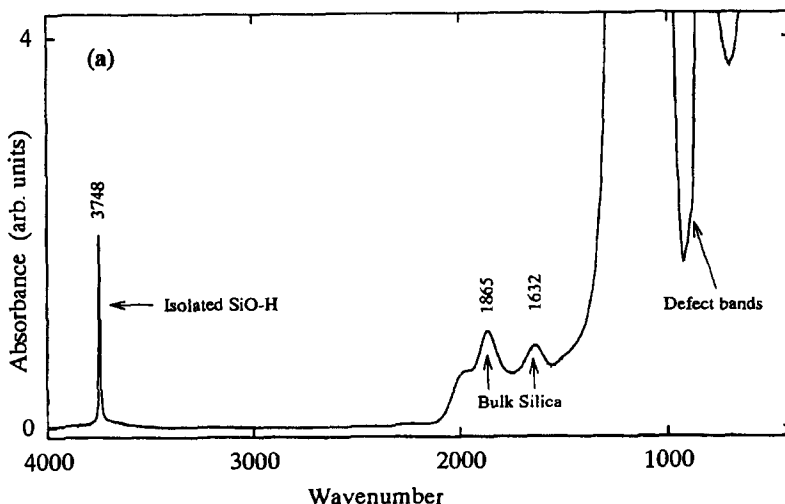


Fig. 19. FTIR spectrum of Surface I (originally appeared in ref. 66).

conditions do not represent those used in typical CVD experiments, they are a compromise between simulating realistic conditions and gaining useful information. Low-temperature dosing is a gross departure from CVD conditions, but was expected to allow the molecules to be adsorbed intact such that their reactions with the silica surface could be observed. Higher temperature dosing was expected to be more representative of actual CVD conditions, although the lifetime of the adsorbates is expected to be short. It was expected that dosing at higher temperatures such as 200°C would result in such rapid reactions that the lifetime of the species adsorbed would be insufficient for detection by this technique.

Rather than attempt to describe all the results in this area, which will be the subject of a more specific review to be published elsewhere,<sup>72</sup> some of our salient results are summarized here which allow the deduction of specific conclusions. Therefore, this discussion will be confined to the interaction of ( $\beta$ -diketonate)Cu<sup>I</sup>L<sub>n</sub> compounds with Surface I which is the least complicated of the three surfaces since interactions with the isolated surface hydroxyl groups and the strained siloxane rings can be easily identified and rationalized. For example, if an adsorbate interacts with the isolated surface hydroxyl group, the characteristic  $\nu(\text{O—H})$  band at 3748 cm<sup>-1</sup> will be diminished in intensity and a new, broad band at lower energy will emerge. If, on the other hand, the adsorbate does not interact with the isolated surface hydroxyl groups, bands associated with the adsorbate will be observed and the isolated surface hydroxyl group band will be unaffected.

The adsorption of (hfac)Cu(PMe<sub>3</sub>) on Surface I at -50°C results in interaction with the isolated surface hydroxyl group as shown in Fig. 20.<sup>73</sup> The intensity of the isolated surface hydroxyl group is significantly diminished and a new broad hydroxyl band, characteristic of a hydrogen bonding interaction is apparent centred at ~3350 cm<sup>-1</sup>. Bands associated with the ring vibrations of the hfac ligand can be discerned between ~1700 and 1350 cm<sup>-1</sup> and the  $\nu(\text{C—H})$  bands associated

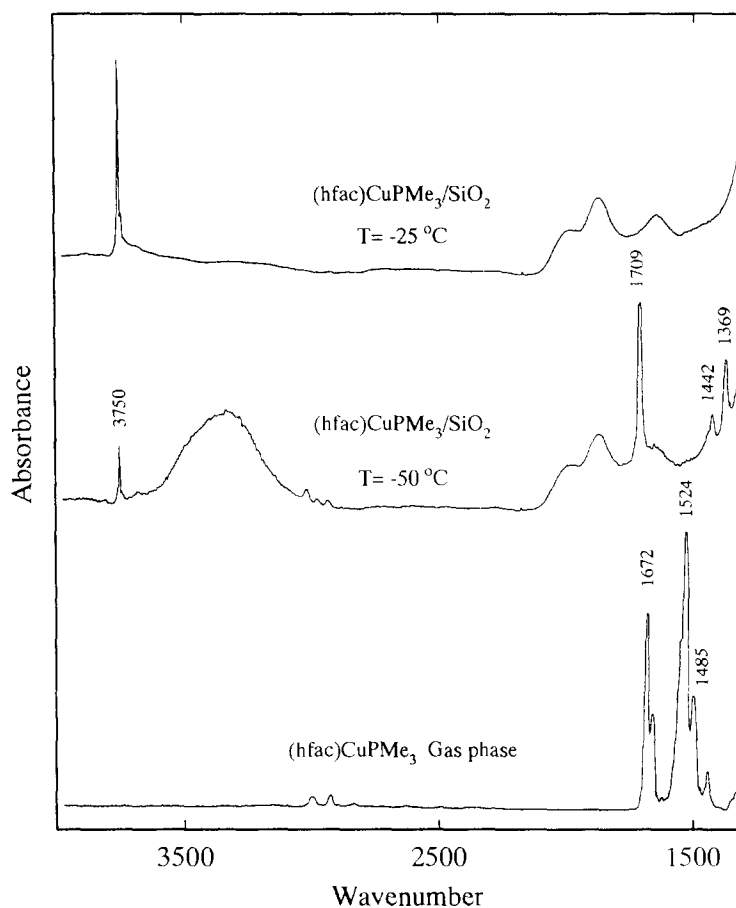


Fig. 20. FTIR spectra of (hfac)Cu(PMe<sub>3</sub>). Middle: Surface I dosed with (hfac)Cu(PMe<sub>3</sub>) at -50°C. Top: after heating to -25°C and Bottom: gas phase FTIR spectrum of (hfac)Cu(PMe<sub>3</sub>).

with  $\text{PMe}_3$  and the central methine of the hfac ligand are apparent at  $\sim 3000 \text{ cm}^{-1}$ . On heating to  $-25^\circ\text{C}$ , all the bands associated with the adsorbed  $(\text{hfac})\text{Cu}(\text{PMe}_3)$  disappear and the intensity of the isolated surface hydroxyl group is restored. The compound  $(\text{hfac})\text{Cu}(\text{PMe}_3)$  molecularly desorbed intact from the silica surface. In a control experiment, the interaction of  $\text{PMe}_3$  with the same silica surface was examined under similar dosing conditions. It was observed that  $\text{PMe}_3$  also interacts with the isolated surface hydroxyl group at  $-50^\circ\text{C}$ , and although some  $\text{PMe}_3$  desorbed on heating, at  $+50^\circ\text{C}$ , some evidence for adsorbed  $\text{PMe}_3$  was still observed. This led us to the conclusion that if the  $\text{Cu}-\text{P}$  bond in  $(\text{hfac})\text{Cu}(\text{PMe}_3)$  was cleaved on adsorption (i.e. chemisorption), then evidence for adsorbed  $\text{PMe}_3$  would be expected at  $-25^\circ\text{C}$ . This may be connected to the selective deposition behaviour observed for  $(\text{hfac})\text{Cu}(\text{PMe}_3)$  indicating that this precursor does not react (i.e. is not chemisorbed) on a silica surface. It is interesting to observe that the modes associated with the hfac ring in  $(\text{hfac})\text{Cu}(\text{PMe}_3)$  are changed dramatically on adsorption compared to the gas-phase FTIR spectrum as shown in Fig. 20. From this observation we deduce that the hfac ring is intimately involved in the adsorption process, such as the interaction proposed in Fig. 21, but in a way which cannot be discerned in detail due to the complex nature of the hfac ring vibrations.

Other copper(I) compounds behave in a quite different fashion as illustrated by the behaviour of  $(\text{hfac})\text{Cu}(\text{2-butyn})$  on Surface I.<sup>64</sup> After dosing  $(\text{hfac})\text{Cu}(\text{2-butyn})$  onto silica at  $25^\circ\text{C}$  under conditions specified in the caption to Fig. 22, the FTIR spectrum provided no evidence for the presence of 2-butyn. This is consistent with a control experiment in which 2-butyn was dosed onto the same surface under similar conditions where no uptake was observed. The adsorbate is also clearly interacting with the isolated surface hydroxyl groups as observed from the change in the appearance of a broad band of slightly lower energy than the isolated surface hydroxyl group stretching frequency. The FTIR spectrum of the remaining adsorbed “ $(\text{hfac})\text{Cu}$ ” is remarkably similar to the FTIR spectrum of the product of the reaction of  $\text{Cu}(\text{hfac})_2$  dosed onto the same surface under similar conditions, as shown in Fig. 22. One interpretation consistent with these

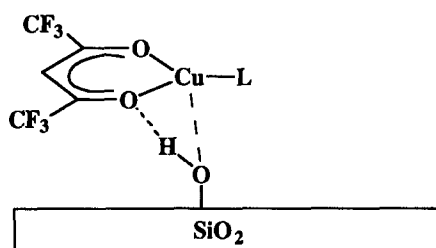


Fig. 21. Proposed interaction between  $(\text{hfac})\text{CuL}$  and isolated surface hydroxyl groups.

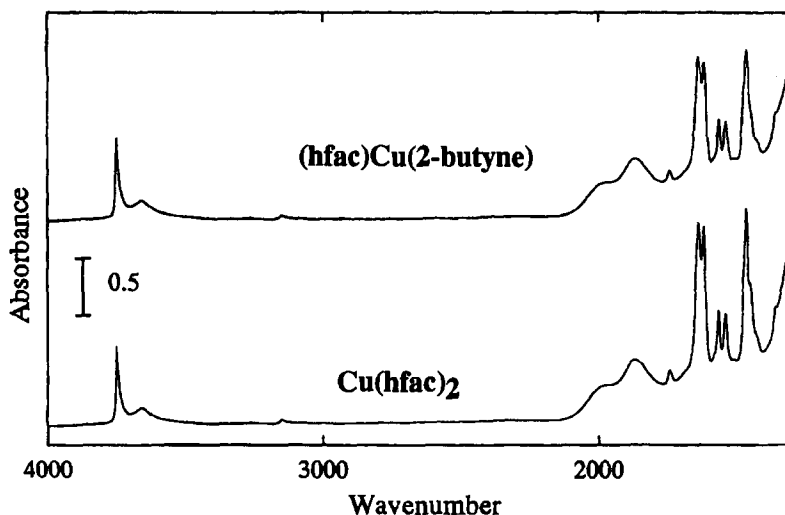


Fig. 22. FTIR spectra of  $(\text{hfac})\text{Cu}(\text{2-butyn})$  and  $\text{Cu}(\text{hfac})_2$  dosed on Surface I (originally appeared in ref. 64).



results is that disproportionation of (hfac)Cu(2-butyne) may occur on the silica surface if two (hfac)Cu species can combine, accounting for the similarity in their FTIR spectra. However, as stated above, it is not necessary that disproportionation occurs on the silica surface. Rather, the (hfac)Cu may decompose by some pathway leading to formation of copper or copper oxides. This result is consistent with the observed non-selective deposition behaviour of (hfac)Cu(2-butyne) because, even at 25°C, it reacts (dissociatively chemisorbs) with silica, presumably forming nuclei capable of further reaction with (hfac)Cu(2-butyne).

One common feature of these reactions on silica is the interaction or reaction of the adsorbate with the surface hydroxyl groups.<sup>17,64 67,73-76</sup> In order to obtain selective deposition (i.e. no deposition on SiO<sub>2</sub>), it is logical to prevent adsorption of (hfac)CuL compounds by removing the reactive surface functionality. This should be achievable by reaction of the surface hydroxyl groups with a silylating agent such as trimethylsilylchloride (TMS-Cl). A number of control experiments were carried out in which silica surfaces were treated with silylating agents and the subsequent uptake of a ( $\beta$ -diketonate)Cu<sup>I</sup>L<sub>n</sub> compound was investigated.<sup>65</sup> One such example is described here for Surface III.<sup>74</sup> Treatment of Surface III, shown in Fig. 23 with TMS-Cl resulted in a reduction in intensity of the isolated surface hydroxyl group intensity and a slight change in the hydrogen-bonded  $\nu(\text{O—H})$  region with the TMS-Cl still present in the gas phase in the cell.

On removing the gaseous species by exposing to dynamic vacuum, it appears that this treatment has removed some isolated surface hydroxyl groups, and the presence of TMS groups is indicated by the  $\nu(\text{C—H})$  bands in the 3000 cm<sup>-1</sup> region. When this surface was treated with (hfac)Cu(VTMS), see Fig. 24, a significant reduction in uptake was observed over the uptake of (hfac)Cu(VTMS) after dosing a non-silylated surface under otherwise identical conditions.

The decrease in uptake of the copper(I) precursor on the passivated silica surface compared to the unpassivated silica surface formed the basis of a series of CVD experiments in which CVD of copper onto passivated and non-passivated silica surfaces was compared. These CVD experiments revealed that under otherwise identical conditions, (hfac)Cu(VTMS) did not deposit copper on

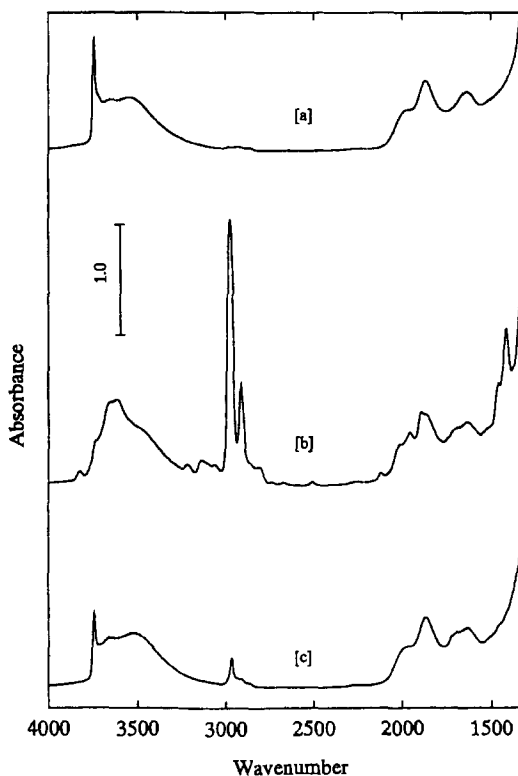


Fig. 23. FTIR data of (a) a Cab-O-Sil surface with isolated and hydrogen-bonded hydroxyl groups present, but with adsorbed water removed, (b) after treatment with 150 mTorr of chlorotrimethylsilane for 15 min at 330 K and (c) after evacuation of the sample chamber (originally appeared in ref. 74).

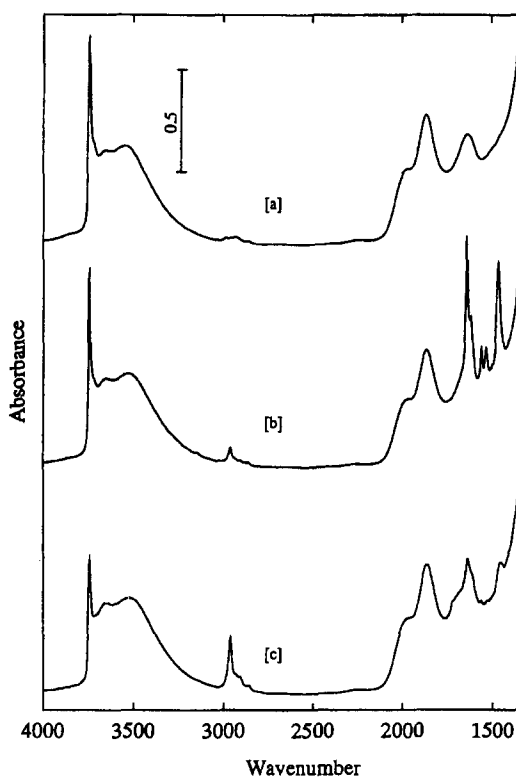


Fig. 24. A comparison between the FTIR spectra for (a) the Cab-O-Sil surface (as prepared in Fig. 2a), (b) the Cab-O-Sil surface dosed with (hfac)Cu(VTMS) (1 mTorr, 10 min, 300 K) and (c) the Cab-O-Sil surface dosed with chlorotrimethylsilane (150 mTorr, 30 min, 330 K) followed by (hfac)Cu(VTMS) (1 mTorr, 10 min, 300 K) (originally appeared in ref. 74).

passivated surfaces, whereas a uniform copper coating was observed on non-passivated silica.<sup>74,75</sup> Figure 25 shows selective deposition of copper onto W in the presence of SiO<sub>2</sub> passivated with hexamethyldisilazane.

There are a number of features of these surface passivation experiments that are interesting to note. We have observed that the reaction of the surface hydroxyl groups with TMS-Cl is not complete below substrate temperatures of 200°C. If the reaction of TMS-Cl with silica surfaces is not complete, then we observe loss in selective deposition of copper with time, presumably because the surface hydroxyl groups are gradually exposed.<sup>75</sup> This problem can be resolved in two ways. The passivating agent can be added during deposition provided it does not react with the copper(I) precursor. It has been demonstrated that this extends the time to loss of selectivity probably because of the higher concentration of the passivating agent compared to the copper(I) precursor and the larger rate constant for the reaction between the passivating agent and the surface hydroxyl groups.<sup>75</sup> The second strategy is to use passivating agents that react completely at lower temperatures. The use of passivating agents with more basic functional groups such as amino groups results in more complete reactions and complete passivation of the silica surface can be achieved under mild conditions in the growth of relatively thick (1 μm) copper films using Me<sub>3</sub>Si-NMe<sub>2</sub> or (Me<sub>3</sub>Si)<sub>2</sub>NH.<sup>65</sup>

It can be seen in the FTIR spectra shown in Fig. 21 that the reaction of TMS-Cl with the surface hydroxyl groups is incomplete, and yet provides sufficient passivation of the surface that the uptake of (hfac)Cu(VTMS) is substantially reduced. This observation leads to the conclusion that the remaining surface hydroxyl groups are not accessible to the copper(I) precursors perhaps as a result of their steric protection. This is especially noticeable in the case of the uptake of (hfac)Cu(VTMS) on silica surfaces prepared at room temperature since it has been demonstrated that this copper(I) species reacts with both isolated and hydrogen-bonded surface hydroxyl groups. The lack of reactivity of the surface towards (hfac)Cu(VTMS) can also be explained by the steric protection of the reactive sites by Me<sub>3</sub>Si groups, especially when one considers that the isolated surface hydroxyl groups are thought to be surrounded by hydrogen-bonded surface hydroxyl groups. If this expla-

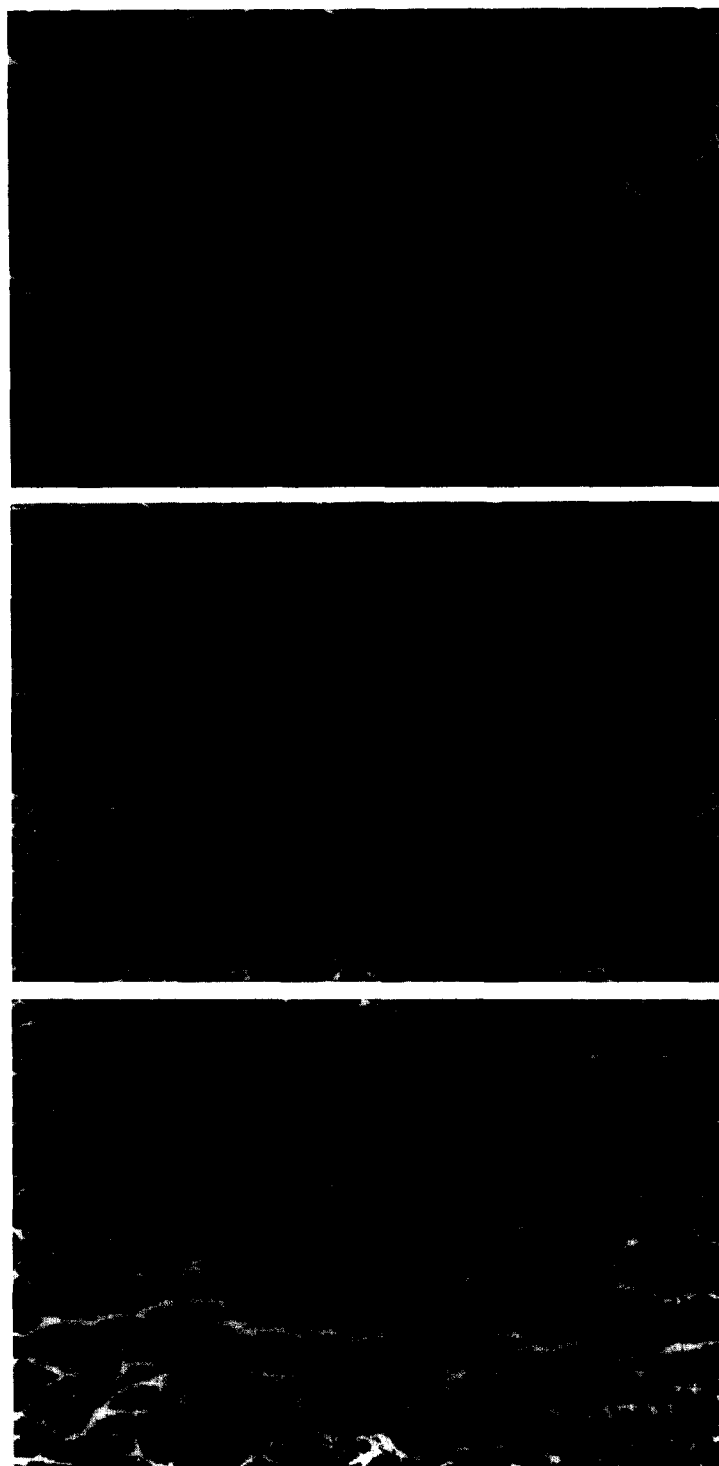


Fig. 25. SEM of a patterned W/silica substrate after passivation with  $(\text{Me}_3\text{Si})_2\text{NH}$  followed by CVD of copper from (hfac)Cu(VTMS) (originally appeared in ref. 75).

nation is correct, then it would be reasonable to use passivating agents that contain more sterically demanding substituents to provide better steric protection of unreacted surface functional groups. The use of  $t\text{-BuCH}_2\text{CH}_2(\text{Me})_2\text{Si-NMe}_2$  was highly effective in passivating silica surface towards reactions with copper(I) precursors.<sup>65</sup> However, one drawback to using more sterically demanding substituents is that their volatility is usually lower and this can cause problems in the efficiency of gas-phase dosing.

#### 4.2. Affect of added reagents during CVD of copper from (hfac)CuL compounds

A number of groups have been investigating the affect of added reagents during the CVD of copper from (hfac)CuL compounds. Gelatos *et al.*<sup>25</sup> deposited copper films by low-pressure CVD from mixtures of (hfac)Cu(VTMS) and water vapour. They observed that the addition of water vapour at the optimum concentration more than doubled the deposition rate and substantially reduced the nucleation time without adversely affecting the copper film resistivity, but excess amounts of water vapour significantly increased the copper resistivity. Auger electron spectroscopy analysis showed no impurities in copper films deposited under optimum water conditions, but oxygen was observed in films deposited under excess water conditions, suggesting copper oxide formation.

We have investigated the influence of added water vapour and hfacH vapour on the CVD of copper from (hfac)Cu(VTMS) and (hfac)Cu(2-butyne).<sup>77</sup> We observed that a small flow rate of water increased the deposition rate by a factor of almost 4 for (hfac)Cu(VTMS) and by a factor of 2 for (hfac)Cu(2-butyne) as shown in Figs 26 and 27. The copper films had a denser morphology and resistivities close to bulk but still contained 1–2% mole fraction of Cu<sub>2</sub>O as determined by X-ray photoelectron spectroscopy (XPS). At higher flow rates the resistivity and the deposition rate deteriorated and SEM showed a surface morphology of poorly connected grains, see Fig. 28. Secondary ionization mass spectroscopy (SIMS) results on films derived from H<sub>2</sub><sup>18</sup>O showed unambiguously that the oxygen in the films was derived from water. The addition of hfacH during the CVD of copper from (hfac)Cu(VTMS) resulted in an enhancement of the deposition rate at low flows, then a dramatic decrease at higher flow rates to a value lower than the deposition rate observed in the absence of hfacH as shown in Fig. 29.

The enhancement of the deposition rate of copper from both (hfac)Cu(VTMS) and (hfac)Cu(2-butyne) combined with the observation that silica surfaces treated with certain passivating agents such as *t*-BuCH<sub>2</sub>CH<sub>2</sub>(Me)<sub>2</sub>Si-NMe<sub>2</sub> are not affected by water<sup>65</sup> suggest that it may be possible to simultaneously increase the copper deposition rate while retaining selective copper CVD.

#### 4.3. STM-defined copper patterns

This surface passivation technique can be extended to other systems and patterning methods. For example, selective CVD of copper has been achieved onto scanning tunnelling microscope (STM)-

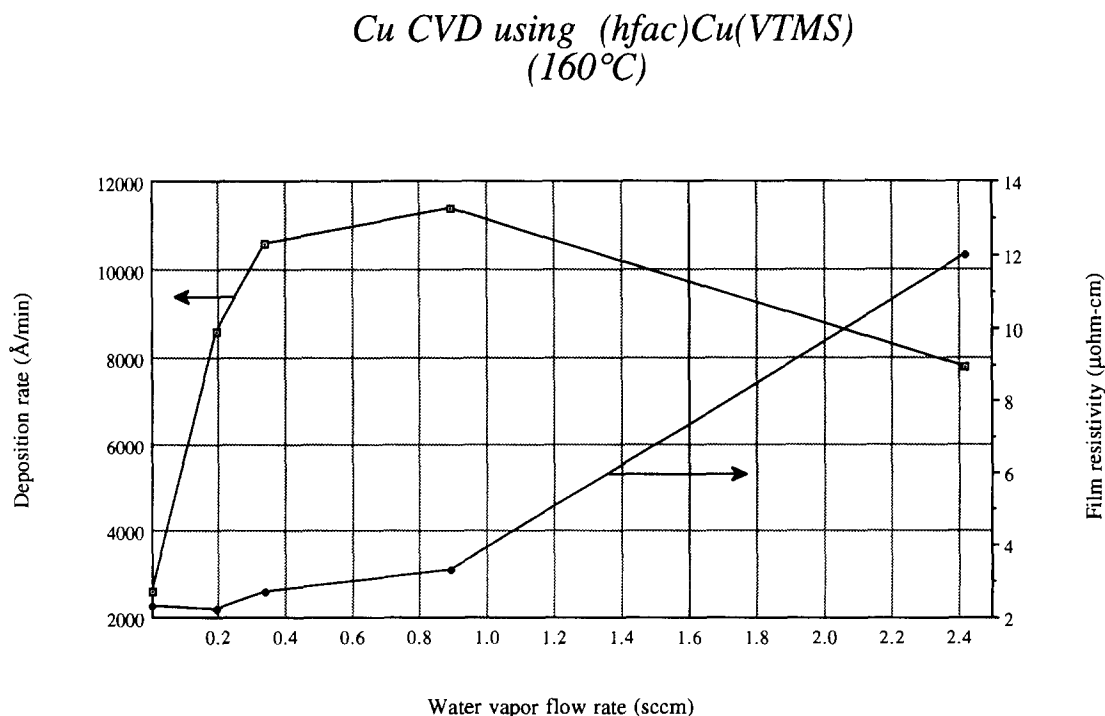


Fig. 26. Plot of deposition rate and film resistivity *vs* water vapour flow rate for (hfac)Cu(VTMS) at 160°C.

*Cu CVD using (hfac)Cu(2-butyne)*  
(150°C)

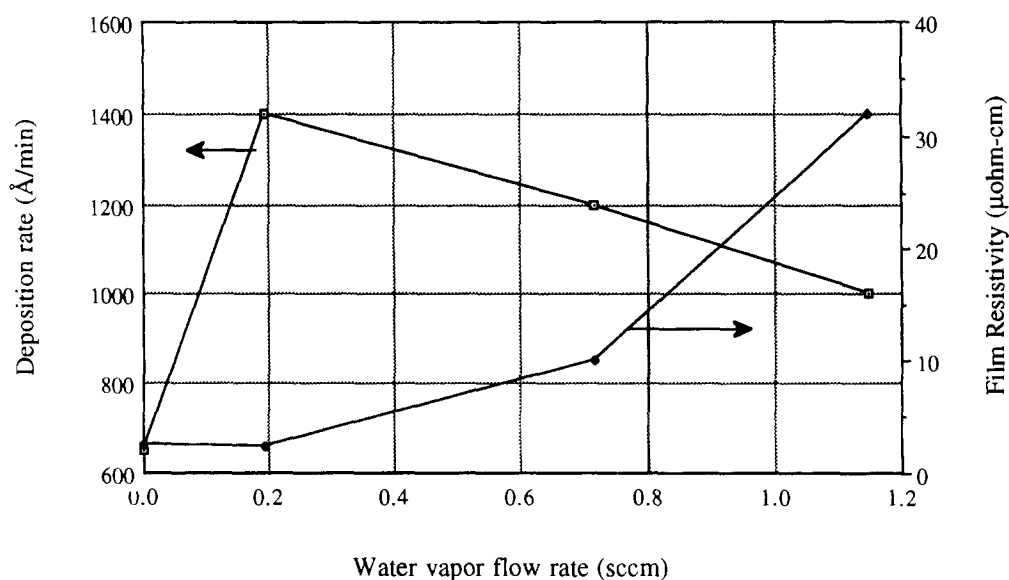


Fig. 27. Plot of deposition rate and film resistivity *vs* water vapour flow rate for (hfac)Cu(2-butyne) at 150°C.

defined patterns in self-assembled monolayers on gold substrates. The formation of patterned copper films comprised of three steps, substrate modification, STM lithography and CVD as shown schematically in Fig. 30.<sup>78,79</sup>

A self-assembled monolayer resist was prepared using octadecyl mercaptan,  $\text{HS}(\text{CH}_2)_{17}\text{CH}_3$ , confined to a Au(111) substrate. The resist was then patterned by using the tip of an appropriately biased STM resulting in selective removal (or modification) of the resist in the area exposed to the tip. The substrate was then subjected to CVD of copper from (hfac)Cu(1,5-COD) at 120°C to produce copper features only in the areas exposed to the tip and not on the unexposed alkyl thiolate resist. This resulted in the formation of critical features having dimensions ranging from 0.05 to 5.0  $\mu\text{m}$ . An example of a high-resolution SEM micrograph showing the presence of a 50 nm copper line is shown in Fig. 31. This method of patterning provides an alternative to high-energy electron- and ion-beam, X-ray and deep UV methods for the formation of submicrometer scale features in polymer resists. In this case, this method relies on patterning of the passivation layer rather than selective reaction of a passivating agent with the non-growth surface to achieve patterned metal films.

#### 4.4. Selective deposition onto patterned Teflon substrates

The deposition of copper onto organic polymer substrates is important because these substrates have low dielectric constants and may be incorporated into future circuit designs. The combination of the low dielectric constant of fluoropolymers such as poly(tetrafluoroethylene) (PTFE) and the high conductivity of copper are highly desirable for optimizing circuit performance. However, the chemical and physical inertness of fluoropolymer surfaces makes them difficult to metallize.

In order to metallize PTFE surfaces by CVD, the PTFE must be rendered reactive towards the precursors and patterned at high resolution. There are a number of methods by which this may be achieved. We have investigated methods which rely on surface modification as shown in Fig. 32.<sup>80-82</sup>

In both variations, sodium naphthalenide is used to activate the PTFE surface while patterning is achieved by X-rays, electron beams or laser irradiation. In variation (A), the PTFE substrate is

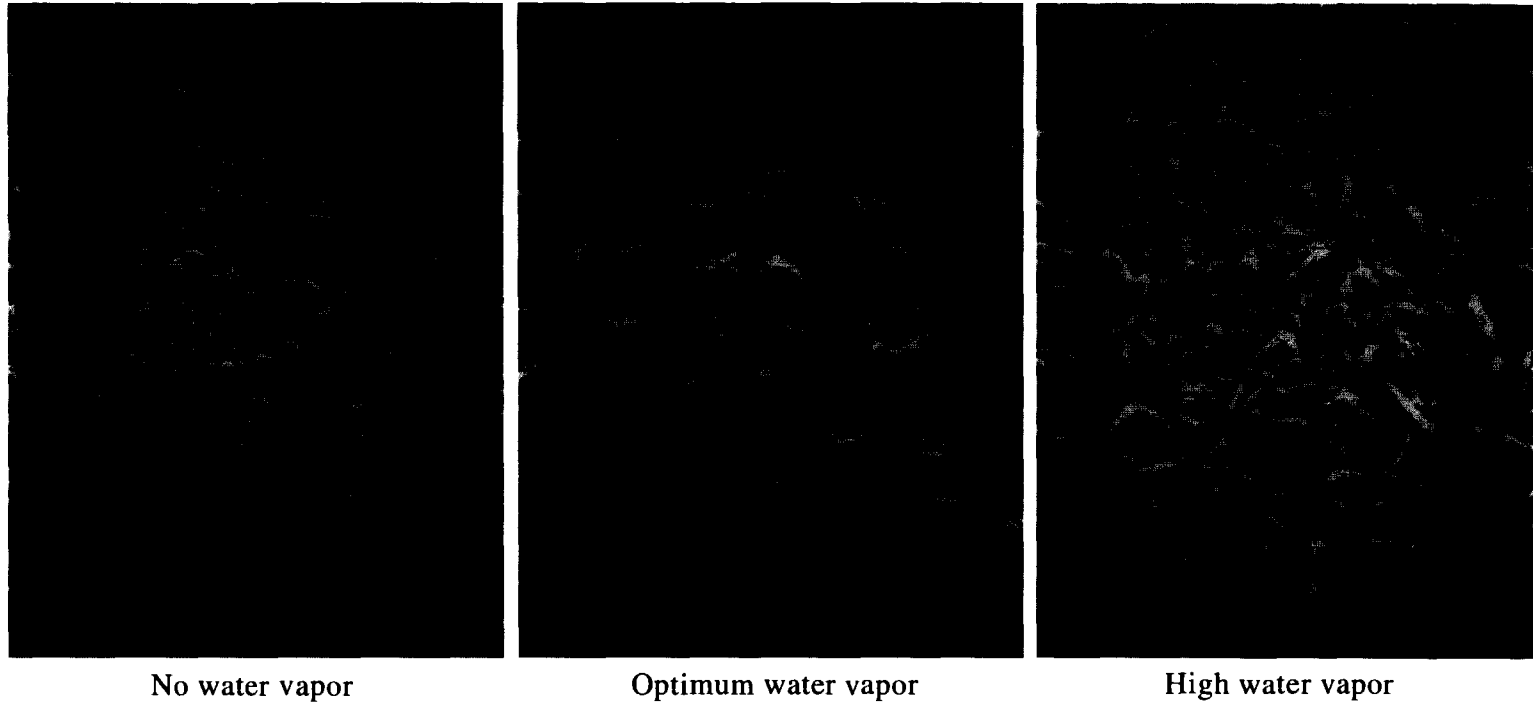


Fig. 28. SEM data showing influence of water vapour flow rate on copper film surface morphology.

*Cu CVD using (hfac)Cu(VTMS)*  
(160°C)

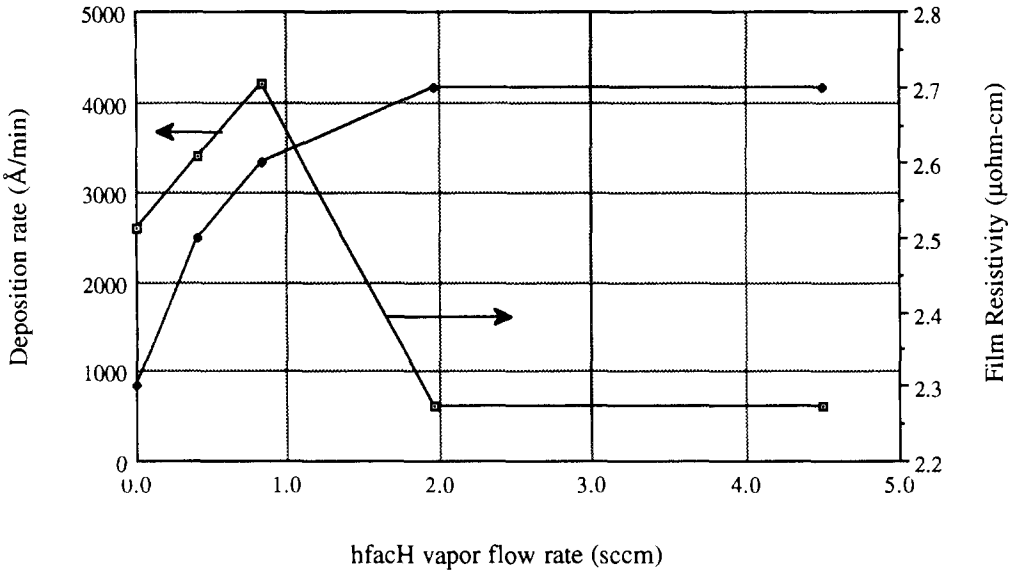
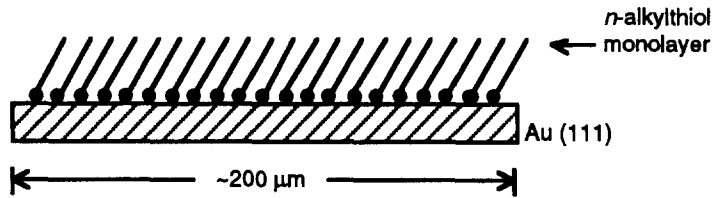
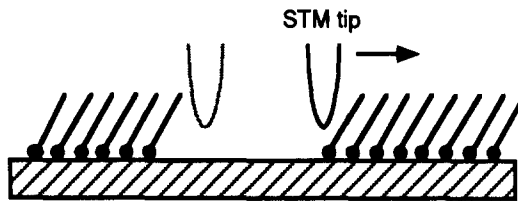


Fig. 29. Plot of deposition rate and film resistivity vs hfach vapour flow rate for (hfac) Cu(VTMS) at 160°C.



**STM Lithography**



**Chemical Vapor Deposition**

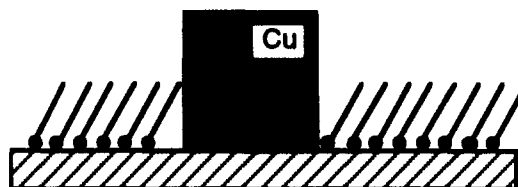


Fig. 30. Schematic representation of selective CVD of copper into STM-defined patterns (originally appeared in ref. 79).



Fig. 31. SEM micrograph of a copper line derived from selective CVD of copper into a STM-derived pattern (originally appeared in ref. 79).

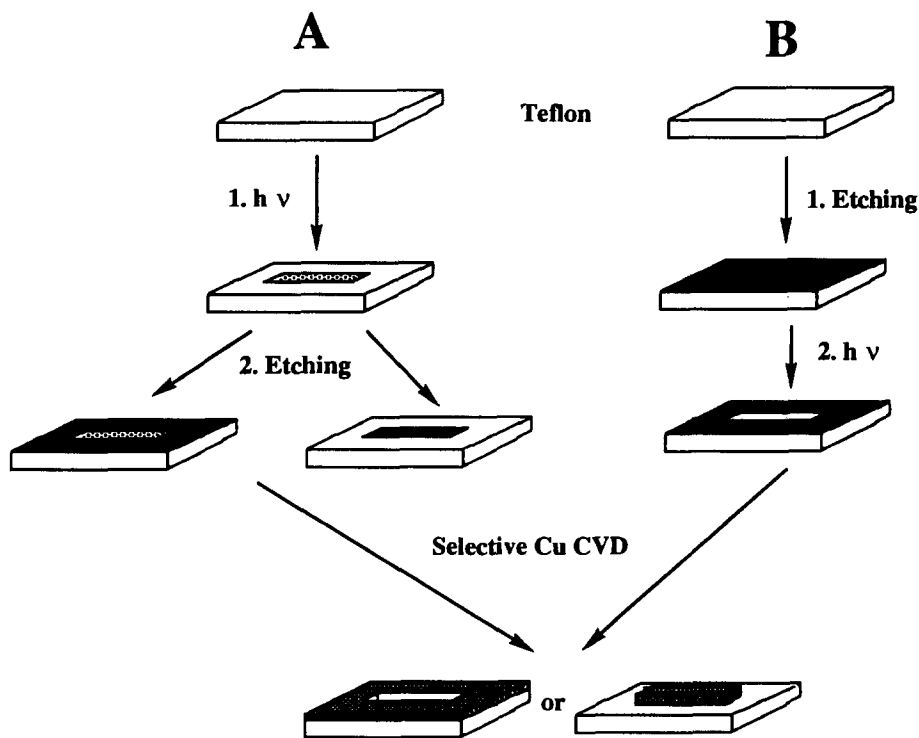


Fig. 32. Overview of methods for selective metallization of PTFE.

first irradiated with either X-rays or electrons to produce a pattern by direct writing in the case of electron beams, or through a mask in the case of X-rays. This process is thought to cross-link and chemically reduce the PTFE surface. In the second step, the PTFE is reacted with a THF solution of sodium naphthalenide which does not significantly affect the irradiated areas of the PTFE surface (they remain white), but reacts significantly with the unmodified PTFE surface (changes colour to brown or black) with defluorination.<sup>83-85</sup> Therefore, this step “develops” the pattern on the substrate which after washing and drying is placed in a hot-wall CVD reactor where copper is deposited using



(hfac)CuL precursors. This results in selective CVD of copper onto the areas of the substrate affected by chemical etching. This process is illustrated schematically in Fig. 33.

In variation (B), the substrate is first reacted with sodium naphthalenide and then a pulsed or CW laser is used to selectively remove portions of the black surface leaving clean (white) Teflon exposed. This patterned surface is then used as a substrate for selective CVD as described above (Fig. 34).

Both variations of this approach rely on irradiation of the substrate with either X-rays, electrons or laser photons to produce the pattern by modifying the polymer surface structure. The surface modification using sodium naphthalenide renders the surface *reactive* towards copper(I) molecules and makes it rough resulting in good *adhesion* of the vapour deposited metal film. Copper films deposited by both methods exhibit good adhesion and low resistivities.

## 5. FORMATION OF PATTERNED FILMS BY ALTERNATIVE METHODS

Patterned metal films can be formed by a variety of other methods in addition to selective CVD. Chemical-mechanical polishing (CMP) and dry etching are in general the most promising. For copper, dry etching has received little attention due to the difficulty in achieving high etching rates at relatively low temperatures in plasma reactors. However, dry cleaning of reactors for removal of copper deposited on the back side of wafers and other hot surfaces does not have the constraint of requiring anisotropic etching and has received significant attention. This problem can be addressed by a chemical approach in which the copper film is first oxidized and then reacted with an appropriate reagent to form a volatile, low-molecular weight species which can then be removed rapidly from the substrate surface. A number of strategies have been adopted to promote copper etching including comproportionation and chemical oxidation followed by de-oligomerization<sup>86</sup> according to eqs (5)–(7). This subject was reviewed recently and the reader is referred to these sources for details.<sup>46,87</sup>

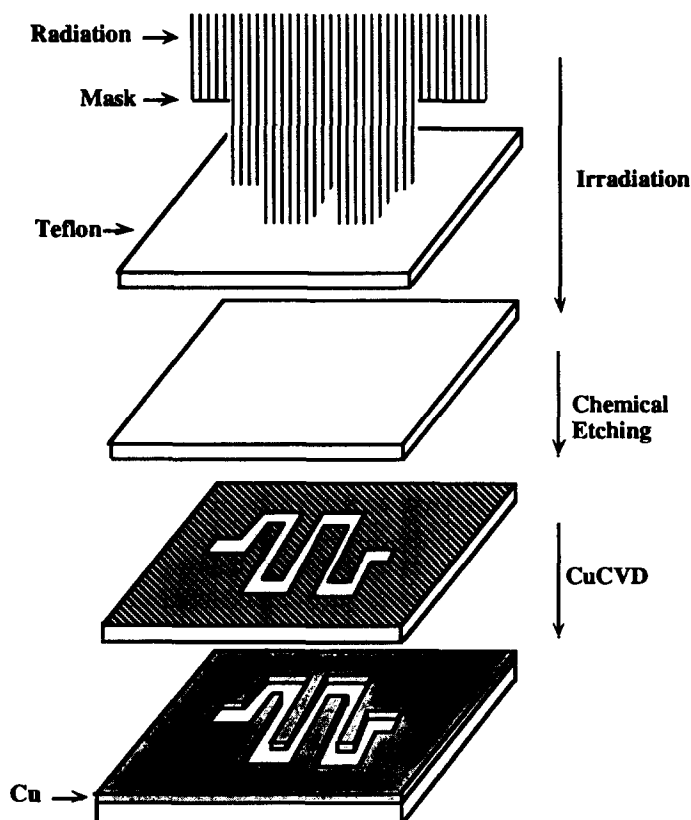


Fig. 33. Schematic representation of the selective metallization using X-ray radiation.

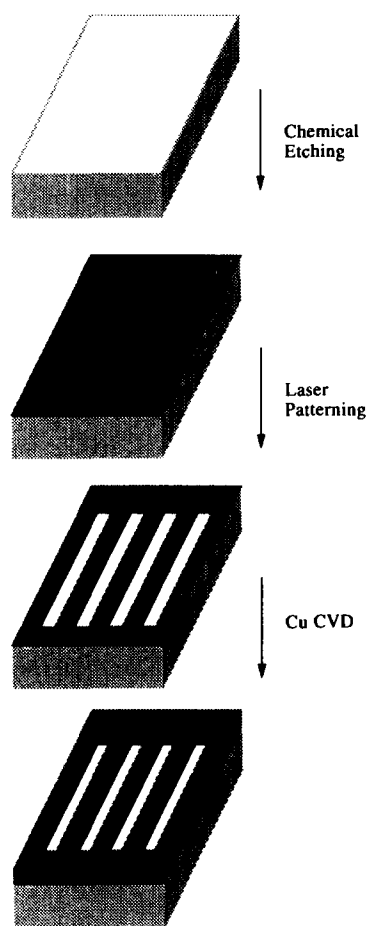
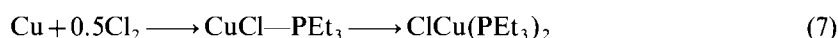
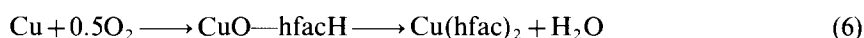
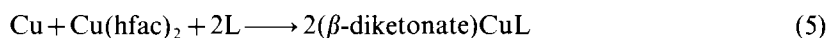


Fig. 34. Schematic representation of the selective metallization using laser radiation.



The approach given in eq. (6) is the most robust.<sup>88</sup> Only simple reagents ( $\text{O}_2$  and hfacH) and processing conditions are required, and rates of  $1 \mu\text{m min}^{-1}$  are easily obtained at temperatures of  $200\text{--}300^\circ\text{C}$ . This approach is also interesting because it allows the removal of a variety of other metal oxides from surfaces.

## 6. PRECURSOR DELIVERY AND METAL ALLOYS

One of the major limitations associated with CVD is the relatively low volatility of metal-containing compounds that are suitable precursors. This probably represents one of the major drawbacks associated with CVD in general and is often the limiting factor in the high rate deposition of many films. It would be valuable to develop a method to enable deposition of films from a wider variety of metal containing compounds in terms of both their thermal stability and their volatility. This problem is being addressed for the case of CVD of metals in a number of groups by developing alternative methods of precursor delivery.<sup>18,89-91</sup>

Conventional delivery methods rely on heating a precursor to achieve a reasonable vapour pressure, limited by the equilibrium vapour pressure of the precursor, for long periods of time. This is problematic because the precursor must then have long term thermal stability at a raised temperature (but react rapidly at higher temperatures) and exhibit a significant vapour pressure. These requirements are both hard to fulfill. An alternative is to introduce the precursor by a different

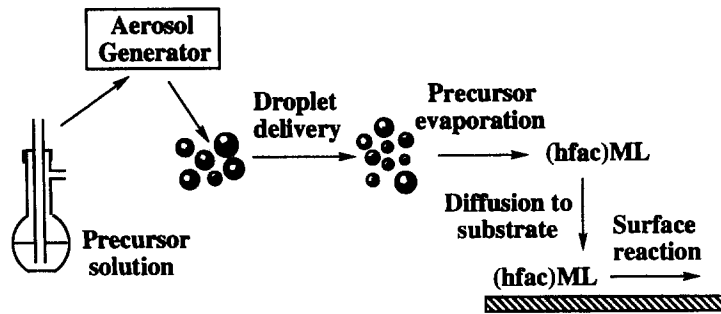


Fig. 35. Fundamental steps in AACVD of (hfac)CuL compounds (originally appeared in ref. 89).

method such as a liquid delivery method which allows for a higher mass throughput per unit time than can be achieved based on the equilibrium vapour pressure of the precursor per unit time. This changes the precursor requirement slightly to alleviate the requirement for volatility at low temperatures and add the requirement of solubility in a solvent that does not interfere in the surface reaction.

Introduction of the precursor based on liquid delivery has been achieved by a number of different methods. Spraying the precursor solution on a preheating surface before introduction into the CVD chamber causes evaporation of the solvent and the precursor but can also lead to some decomposition which is undesirable. Supercritical fluid transport (SFT) has also been used to deposit metal films, but is limited by the availability of suitable solvents and their compatibility with metal-containing compounds.<sup>91</sup> We have chosen to study a liquid delivery method which involves the generation of an aerosol of the precursor solution which facilitates high evaporation rates in the CVD reactor due to the small size of the aerosol droplets. The fundamental steps involved in aerosol-assisted (AA) CVD of a metal-containing compound such as (hfac)CuL are presented in Fig. 35.<sup>89</sup> A variety of materials have been deposited by this method.<sup>92-95</sup> This delivery method has a number of advantages over traditional delivery methods which include: (i) higher deposition rates should be possible as a result of the higher mass transport of the precursor to the substrate; (ii) compounds with lower thermal stability and lower volatility can be used; (iii) the reproducible deposition of complex stoichiometry films should be possible by mixing precursors that are compatible with each other and the solvent system. These three points are illustrated in Figs 36-38. Figure 36 shows the results of a comparison of the CVD and AACVD of copper from (hfac)Cu(1,5-

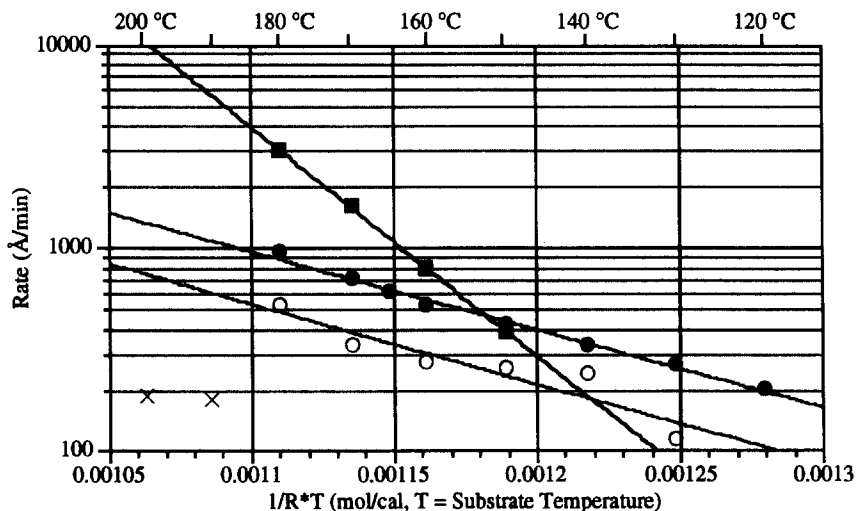


Fig. 36. Plots of log of deposition rate vs  $1/RT$  ( $T$  = substrate temperature) for AACVD at preheating temperatures of 60°C for nozzle-substrate distance of 0.7 cm (●) and 1.7 cm (○) and for traditional warm-wall (88°C) CVD at 10 mTorr (◆) (originally appeared in ref. 89).

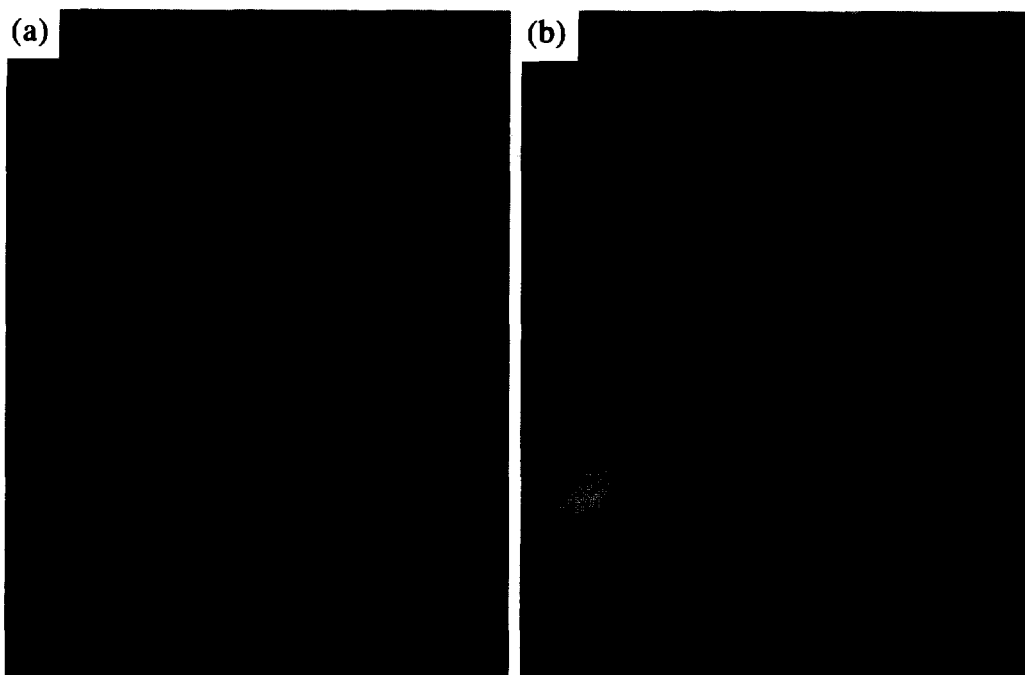


Fig. 37. SEM of two Ag films deposited by AACVD of (hfac)Ag(SET) on Cu substrates at a preheating temperature of 80°C and substrate temperatures of (a) 120°C and (b) 200°C (originally appeared in ref. 89).

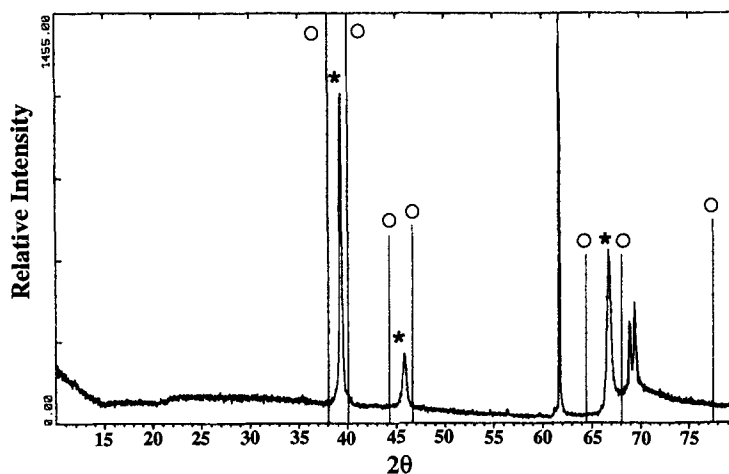


Fig. 38. Powder X-ray diffraction data for the film Ag/Pd alloy deposited by AACVD of (hfac)Ag(SET) and Pd(hfac)<sub>2</sub> in the presence of H<sub>2</sub> (originally appeared in ref. 89).

COD) which resulted in higher deposition rates at lower temperatures and a change in mechanism as evidenced by the difference in the slope of the Arrhenius plot.<sup>89</sup> Figure 37 shows the SEM data for a high-purity (as determined by XPS) low-resistivity, silver film derived from AACVD of (hfac)Ag(SET)<sub>2</sub>.<sup>90,96,97</sup> This precursor cannot be sublimed intact, even though it is monomeric in the solid state (see Fig. 39), and therefore is unsuitable for CVD using conventional delivery methods because it cannot be transported to the CVD reactor. Finally, Fig. 38 shows the powder X-ray diffraction pattern of a crystalline Ag/Pd alloy film which was deposited by AACVD from (hfac)Ag(SET)<sub>2</sub> and Pd(hfac)<sub>2</sub> showing that crystalline binary alloy films can be deposited reproducibly at low temperatures.<sup>90</sup> Furthermore, the composition of the film varies in a close relationship with the composition of the solution. A plot of the powder X-ray diffraction data shown in Fig. 40 for films obtained as a function of ratio of silver(I) and palladium(II) precursors shows a systematic variation in film composition.

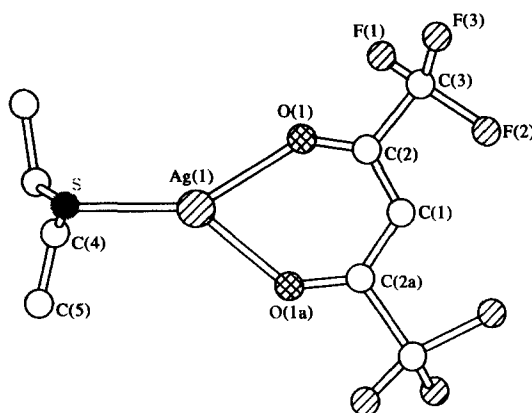


Fig. 39. Solid-state molecular structure of (hfac)Ag(SEt<sub>2</sub>) as determined by single-crystal X-ray diffraction.

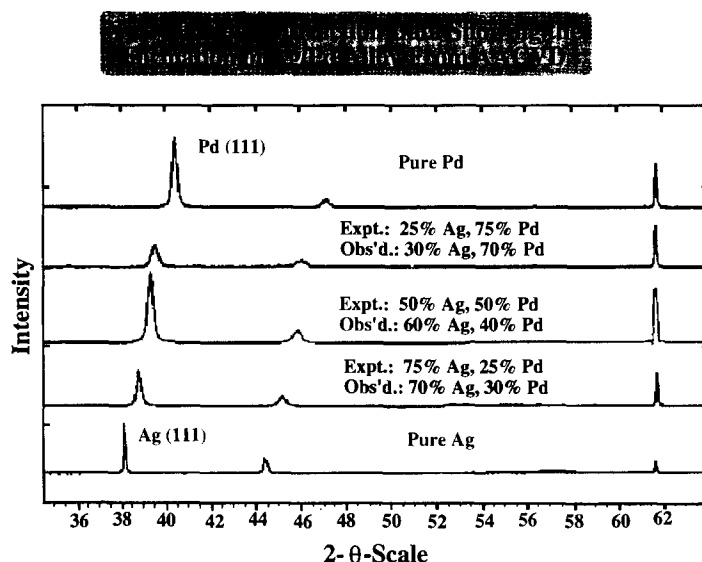
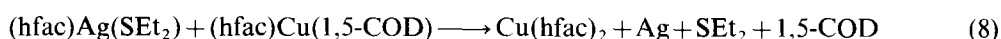


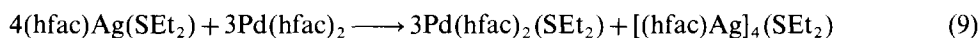
Fig. 40. Powder X-ray diffraction data for the film Ag/Pd alloy deposited by AACVD of (hfac)Ag(SEt) and Pd(hfac)<sub>2</sub> in the presence of H<sub>2</sub> as a function of solution composition.

There are some possible drawbacks to this method of precursor delivery if the appropriate care in precursor and solvent selection is not taken. It is important that the solvent should not be cleaved during the deposition experiment such that it ultimately leads to contamination of the growing film. In the systems we have examined, it appears that toluene is not cleaved based on the characterization data (purity and resistivity) of the films deposited. In the deposition of binary or more complex materials, it is desirable to avoid reactions between the precursors which may result in the formation of lower volatility species. In some cases we have observed a rapid reaction between pairs of metal organic complexes as is the case for (hfac)Ag(SEt<sub>2</sub>) and (hfac)Cu(1,5-COD) which we attribute to the pathway shown in eq. (8). This problem can be avoided by choosing alternative reagents which do not react at ambient temperature such as (hfac)Ag(SEt<sub>2</sub>) and Cu(hfac)<sub>2</sub>.



In other cases, such as that described above for mixtures of (hfac)Ag(SEt<sub>2</sub>) and Pd(hfac)<sub>2</sub>, a reaction occurs on a slower timescale which we believe allows for film deposition from the original species, but illustrates the need to investigate the chemistry of each system individually. The reaction of eq.

(9) results in the formation of two new species, each of which have been unambiguously characterized as shown in Figs 41 and 42 which shows that the silver(I) product is oligomeric in the solid state.



In spite of these concerns, we believe that AACVD may provide a method which avoids the requirement of high precursor volatility in the design of metal-containing precursors that is difficult to fulfill as outlined above.

## 7. CONCLUSIONS AND FUTURE DIRECTIONS

The CVD of copper via disproportionation of copper(I) compounds leads to the deposition of high-quality copper films. The high purity of the films is probably associated with this reaction pathway since no thermal decomposition of the supporting ligands is required. We had originally

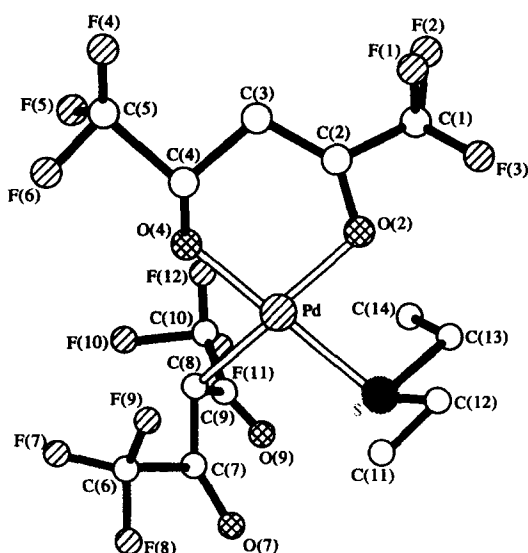


Fig. 41. Solid-state molecular structure of Pd(hfac)<sub>2</sub>(SEt)<sub>2</sub> as determined by single-crystal X-ray diffraction.

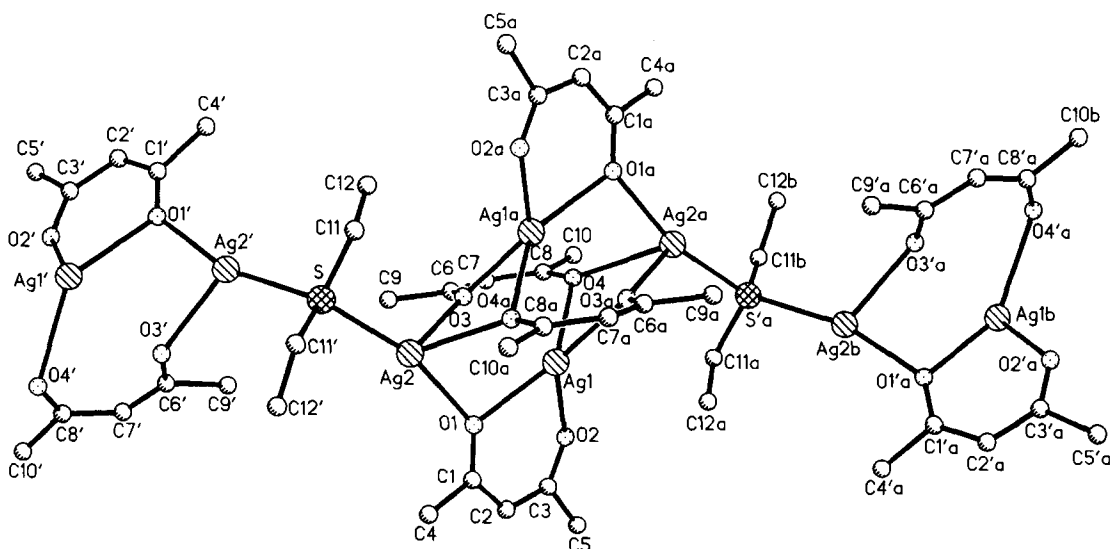


Fig. 42. Solid-state molecular structure of [(hfac)Ag]<sub>2</sub>(SEt)<sub>2</sub> as determined by single-crystal X-ray diffraction.

envisioned it would be possible to achieve selective deposition of copper through controlled precursor design. While this has been demonstrated for the case of ( $\beta$ -diketonate)Cu(PR<sub>3</sub>) compounds, it is difficult to combine all the desirable precursor properties including high volatility, long shelf life, disproportionation at 200°C, high deposition rates and selective reaction with one surface in the presence of another. The dichotomy between achieving a high degree of selectivity and a high deposition rate is analogous to the development of highly reactive and selective catalysts. If the reactivity is high, the selectivity for a particular organic transformation is generally low, while if the selectivity is high the reactivity is usually low. The selective deposition of high-purity films at high deposition rates by considering precursor design alone is not likely to be effective. Instead, a better strategy is to design the precursor to have a long shelf life but be reactive at elevated temperatures and to control selective deposition through derivatization of the growth and/or non-growth surface to enhance or inhibit surface reactions. Selective deposition through surface passivation of the non-growth surface, as described here for the case of copper, is an example of this strategy (see Fig. 43). Whether this strategy is general and can be extended to the CVD of other materials is of great

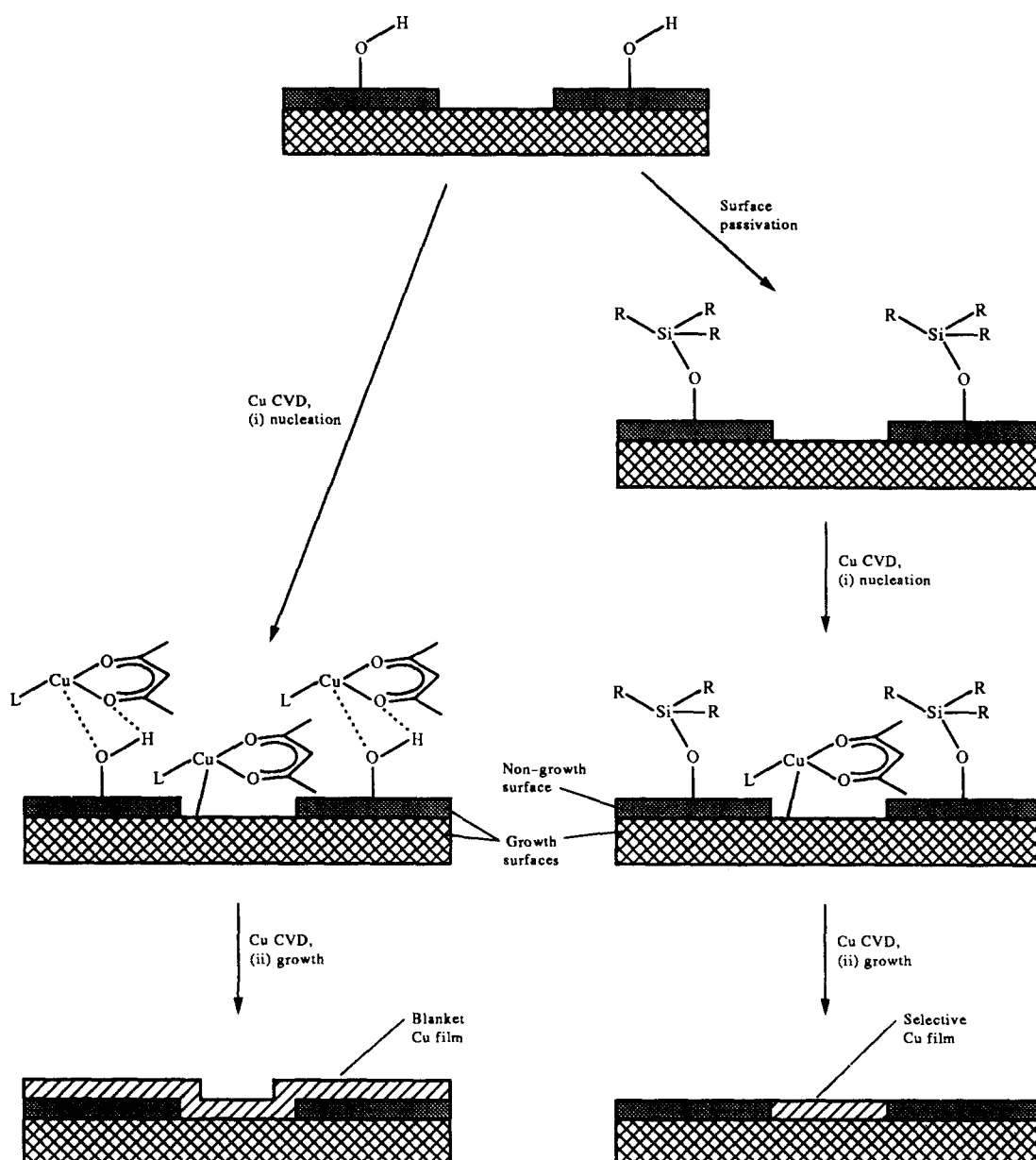


Fig. 43. Overview of selective CVD of copper by surface passivation.

scientific and technological interest and is the subject of future directions. We believe that the AACVD of metals is a valuable method of broadening the variety of metal-containing compounds that can be used as precursors and this method will be particularly useful for the formation of metal alloys. Furthermore, it may be possible to combine selective deposition via surface modification with AACVD to obtain patterned metal films at high deposition rates.

Many aspects of the CVD of metals have yet to be understood. Many metals have not yet been deposited at high rates in high purity at low temperatures because of the lack of suitable precursors.<sup>1</sup> Even in these cases, little is usually known about the reaction mechanisms leading to film formation. Reliable selective CVD has been demonstrated only in a few cases (Cu, Al, W). For these reasons and because of the many important applications of CVD of metals, this is likely to be an area of intense research interest over the next few years.

*Acknowledgments*—We thank the National Science Foundation (#CHE-9107035 and #CTS 9058538), the Office of Naval Research, Sandia National Laboratories, Spectrum CVD, Motorola and Sharp Microelectronic Technologies Inc. For funding parts of this research. We are grateful for the contributions of Professor Kai-Ming Chi, Dr Janos Farkas, Dr Hyun-Kook Shin, Mr Tom Corbitt, Mr Ajay Jain, Dr Christophe Roger, Mr Chong Ying Xu, Mr Alec Bailey and collaborations with Professor R. M. Crooks, Mr Jon Schoer and Ms C. Ross. Mark Hampden-Smith also thanks Drs Phil Harrison (University of Nottingham) and Carole Harrison (Nottingham Trent University) for their hospitality during a Sabbatical stay and the University of Nottingham for a Kipping Fellowship.

## REFERENCES

1. T. T. Kodas and M. J. Hampden-Smith (Eds), *The Chemistry of Metal CVD*. VCH, Weinheim (1994).
2. M. L. Hitchman and K. F. Jensen, *Chemical Vapor Deposition: Principles and Applications*. Academic Press, San Diego, CA (1993).
3. D. W. Hess and K. F. Jensen, *Microelectronics Processing*. American Chemical Society, Washington, D.C. (1989).
4. W. L. Gladfelter, *Chem. Mater.* 1993, **5**, 1372.
5. S. Wolf and R. N. Tauber, *Silicon Processing for the VLSI Era*. Lattice Press, Sunset Beach, CA (1987).
6. R. Jaraith, A. Jain, R. D. Tolles, M. J. Hampden-Smith and T. T. Kodas, in *The Chemistry of Metal CVD: Chapter 1* (Edited by T. T. Kodas and M. J. Hampden-Smith). VCH, Weinheim (1994).
7. Z. Y. Li, H. Maeda, K. Kusakabe, S. Morooka, H. Anzai and S. Akiyama, *J. Membrane Sci.* 1993, **78**, 247.
8. J. Shu, B. P. A. Grandjean, A. Van Neste and S. Kalaguine, *Can. J. Chem. Engng* 1991, **69**, 1036.
9. D. Wu, R. A. Outlaw and R. L. Ash, *J. Appl. Phys.* 1993, **74**, 4990.
10. J. Li, R. Blewer and J. W. Mayer, (Eds), *Copper Metallization*, Vol. XVIII, pp. 18–56. Materials Research Society, Pittsburgh (1993).
11. V. T. Kruck and K. Z. Bauer, *Anorg. Allgem. Chem.* 1969, **364**, 551.
12. N. Awaya and Y. Arita, *Digest of Technical Papers* 1989, Section 12–4, 103.
13. N. Awaya and Y. Arita, in *Adv. Met. for ULSI Appl.*, Vol. V, pp. 231. Materials Research Society, Pittsburgh (1991).
14. N. Awaya and Y. Arita, *Jpn J. Appl. Phys. Pt 1* 1993, **32**, 3915–3919.
15. Y. Chang, in *Mat. Res. Soc. Symp. Proc.*, Vol. 282, pp. 335. Materials Research Society, Pittsburgh (1993).
16. S. J. Fine, P. N. Dyer, J. A. T. Norman, B. A. Muratore and R. L. Iampietro, in *Mat. Res. Soc., Symp. Proc.*, Vol. 204, pp. 415. Materials Research Society, Pittsburgh (1990).
17. P. M. Jefferies, L. H. Dubois and G. S. Girolami, *Chem. Mater.* 1992, **4**, 1169.
18. A. E. Kaloyeros, A. Feng, J. Garhart, K. C. Brooks, S. K. Gosh, A. N. Saxena and F. Luethrs, *J. Electronic Mater.* 1990, **19**, 271.
19. B. Lecohier, B. Calpini, J. M. Philippoz, H. van den Bergh, D. Laub and P. Buffat, *J. Electrochem. Soc.* 1993, **140**, 789–796.
20. B. Lecohier, B. Calpini, J. M. Philippoz and H. van den Bergh, *J. Appl. Phys.* 1992, **72**, 2022–2026.
21. A. Maverick and G. L. Griffin, in *The Chemistry of Metal CVD: Chapter 4* (Edited by T. T. Kodas and M. J. Hampden-Smith). VCH, Weinheim (1994).
22. W. Rees, in *Mat. Res. Soc. Symp. Proc.*, Vol. 250, pp. 297. Materials Research Society, Pittsburgh (1992).
23. V. L. Young, D. F. Cox and M. E. Davis, *Chem. Mater.* 1993, **5**, 1701.
24. D. Temple and A. Reisman, *J. Electrochem. Soc.* 1989, **136**, 3525.
25. A. V. Gelatos, R. Marsh, M. Kottke and C. J. Mogab, *Appl. Phys. Lett.* 1993, **63**, 2842–2844.
26. D. H. Kim, R. H. Wentorf and W. N. Gill, *J. Appl. Phys.* 1993, **74**, 5164–5166.



27. D. H. Kim, R. H. Wentorf and W. N. Gill, *J. Electrochem. Soc.* 1993, **140**, 3267–3272.
28. D. H. Kim, R. H. Wentorf, and W. N. Gill, *J. Electrochem. Soc.* 1993, **140**, 3273–3279.
29. H.-K. Shin, K. M. Chi, M. J. Hampden-Smith, T. T. Kodas, J. D. Farr and M. Paffett, in *Mat. Res. Soc. Symp. Proc., Fall MRS Meeting, Symposium E* (1990).
30. H.-K. Shin, M. J. Hampden-Smith, T. T. Kodas and E. N. Duesler, *Polyhedron* 1990, **6**, 645.
31. H. K. Shin, K.-M. Chi, M. J. Hampden-Smith, T. T. Kodas, M. F. Paffett and J. D. Farr, *Chem. Mater.* 1992, **4**, 788.
32. A. Jain, K.-M. Chi, M. J. Hampden-Smith, T. T. Kodas, M. F. Paffett and J. D. Farr, *J. Mater. Res.* 1992, **7**, 261.
33. A. Jain, K.-M. Chi, M. J. Hampden-Smith, T. T. Kodas, M. F. Paffett and J. D. Farr, *Chem. Mater.* 1991, **3**, 995.
34. S. L. Cohen, M. Liehr and S. Kasi, *Appl. Phys. Lett.* 1992, **60**, 50.
35. J. A. T. Norman, B. A. Muratore, P. N. Dyer, D. A. Roberts and A. K. Hochberg, *J. Physique* 1992, **IV**, 1, C2–271.
36. R. Kumar, A. W. Maverick, F. R. Fronczek, W. G. Lai and G. L. Griffin, in *200th American Chemical Society Meeting*, Atlanta (1991).
37. R. Nast, R. Mohr and R. C. Schultze, *Chem. Ber.* 1963, **96**, 2127.
38. R. Nast and W.-H. Lepel, *Chem. Ber.* 1969, **102**, 3224.
39. W. A. Anderson, A. J. Carty, G. J. Palenik and G. Schreiber, *Can. J. Chem.* 1971, **49**, 761.
40. R. J. Restivo, A. Costin, G. Ferguson and A. J. Carty, *Can. J. Chem.* 1975, **53**, 1949.
41. G. Doyle, K. A. Eriksen and D. Van Engen, *Organometallics* 1985, **4**, 830.
42. H.-K. Shin, M. J. Hampden-Smith, T. T. Kodas and E. N. Duesler, *Can. J. Chem.* 1992, **70**, 2954.
43. H. K. Shin, K. M. Chi, J. Farkas, M. J. Hampden-Smith, T. T. Kodas and E. N. Duesler, *Inorg. Chem.* 1992, **31**, 424.
44. K.-M. Chi, H. K. Shin, M. J. Hampden-Smith, T. T. Kodas and E. N. Duesler, *Polyhedron* 1991, **10**, 2293.
45. K.-M. Chi, H. K. Shin, M. J. Hampden-Smith, T. T. Kodas and E. N. Duesler, *Inorg. Chem.* 1991, **30**, 4293.
46. M. J. Hampden-Smith and T. T. Kodas, in *The Chemistry of Metal CVD: Chapter 5* (Edited by T. T. Kodas and M. J. Hampden-Smith). VCH, Weinheim (1994).
47. T. H. Baum, C. E. Larson and G. May, *J. Organomet. Chem.* 1992, **425**, 189.
48. T. H. Baum and C. E. Larson, *J. Electrochem. Soc.* 1993, **140**, 154.
49. T. H. Baum and C. E. Larson, *Chem. Mater.* 1992, **4**, 365.
50. R. Kumar, F. R. Fronczek, A. W. Maverick, G. W. Lai and G. L. Griffin, *Chem. Mater.* 1992, **4**, 577.
51. K. M. Chi, T. S. Corbitt, M. J. Hampden-Smith, T. T. Kodas and E. N. Duesler, *J. Organomet. Chem.* 1993, **499**, 181.
52. K. M. Chi, J. Farkas, M. J. Hampden-Smith, T. T. Kodas and E. N. Duesler, *J. Chem. Soc., Dalton Trans.* 1992, 1113.
53. K. M. Chi, M. J. Hampden-Smith, T. T. Kodas and E. N. Duesler, Unpublished results 1992.
54. H. K. Shin, M. J. Hampden-Smith, T. T. Kodas and E. N. Duesler, *J. Chem. Soc., Chem. Commun.* 1992, 217.
55. W. R. Wolf, R. E. Sievers and G. H. Brown, *Inorg. Chem.* 1972, **11**, 1995.
56. T. T. Kodas and M. J. Hampden-Smith, in *The Chemistry of Metal CVD: Chapter 9* (Edited by T. T. Kodas and M. J. Hampden-Smith). VCH, Weinheim (1994).
57. H. K. Shin, K.-M. Chi, M. J. Hampden-Smith, T. T. Kodas, M. F. Paffett and J. D. Farr, *Angew. Chem. Adv. Mater.* 1991, **3**, 246.
58. S. K. Reynolds, C. J. Smart, E. F. Baran, T. H. Baum, C. E. Larson and P. J. Brock, *J. Appl. Phys. Lett.* 1991, **59**, 2332.
59. A. Jain, K.-M. Chi, M. J. Hampden-Smith, T. T. Kodas, M. F. Paffett and J. D. Farr, *J. Electrochem. Soc.* 1993, **140**, 1434.
60. J. E. Parmeter, *J. Appl. Phys.* 1993, **97**, 11530.
61. J. E. Parmeter and T. R. Omstead, *Advanced Metallization for ULSI Applications* 1993, **ULSI-VIII**, 135.
62. M. E. Gross and V. M. Donnelly, in *Advanced Metallization for ULSI Applications* (Edited by V. S. Rana and R. V. Joshi), p. 355. Materials Research Society, Pittsburgh (1991).
63. K. V. Guinn, V. M. Donnelly, M. E. Gross, F. A. Baiocchi, I. Petrov and J. E. Greene, *Mater. Res. Soc., Symp. Proc.* 1993, **282**, 379.
64. J. Farkas, M. J. Hampden-Smith and T. T. Kodas, *J. Phys. Chem.* 1994, **98**, 6763.
65. J. Farkas, M. J. Hampden-Smith and T. T. Kodas, *J. Electrochem. Soc.* 1994, **141**, 3539.
66. J. Farkas, M. J. Hampden-Smith and T. T. Kodas, *J. Phys. Chem.* 1994, **98**, 6753.
67. J. Farkas, M. J. Hampden-Smith and T. T. Kodas, *J. Electrochem. Soc.* 1994, **141**, 3547.
68. M. L. Hair, *Infrared Spectroscopy in Surface Chemistry*. Marcel Dekker, New York (1967).
69. R. K. Iler, *The Chemistry of Silica*. John Wiley and Sons, New York (1979).

70. B. A. Morrow, in *Spectroscopic Characterization of Heterogeneous Catalysts. Part 57A: Methods of Surface Analysis* (Edited by J. L. G. Fierro), Vol. 57A. Elsevier, Amsterdam (1990).
71. C.-M. Chiang, B. R. Zegarski and L. H. Dubois, *J. Phys. Chem.* 1993, **97**, 6948.
72. J. Farkas, M. J. Hampden-Smith and T. T. Kodas, Manuscript in preparation.
73. F. D. Hardcastle, J. Farkas, C. H. F. Peden, T. R. Omstead, R. S. Blewer, M. J. Hampden-Smith and T. T. Kodas, in *Advanced Metallization for ULSI Applications* (Edited by V. S. Rana and R. V. Joshi), p. 413. Materials Research Society, Pittsburgh (1992).
74. A. Jain, J. Farkas, M. J. Hampden-Smith and T. T. Kodas, *Appl. Phys. Lett.* 1992, **62**, 2662.
75. A. Jain, R. Jaraith, T. T. Kodas and M. J. Hampden-Smith, *J. Vac. Sci. Technol. B* 1993, **11**, 2107.
76. L. H. Dubois, *J. Electrochem. Soc.* 1992, **139**, 3295.
77. A. Jain, J. Farkas, M. J. Hampden-Smith and T. T. Kodas, *Spring MRS Meeting* (1994).
78. T. S. Corbitt, R. M. Crooks, C. B. Ross, M. J. Hampden-Smith and J. K. Schoer, *Angew. Chem. Adv. Mater.* 1993, **5**, 935.
79. T. S. Corbitt, R. M. Crooks, M. J. Hampden-Smith, C. B. Ross and J. K. Schoer, *Langmuir* 1994, **10**, 615.
80. R. Rye, J. A. Knapp, K. M. Chi, M. J. Hampden-Smith and T. T. Kodas, *Appl. Phys.* 1992, **72**, 5941.
81. R. Rye, K. M. Chi, M. J. Hampden-Smith and T. T. Kodas, *J. Electrochem. Soc.* 1992, **139**, L60.
82. M. J. Hampden-Smith, T. T. Kodas and R. R. Rye, *Angew. Chem. Adv. Mater.* 1992, **4**, 524.
83. R. R. Rye and G. W. Arnold, *Langmuir* 1989, **5**, 1331.
84. R. R. Rye, *Langmuir* 1990, **6**, 338.
85. R. R. Rye and N. D. Shinn, *Langmuir* 1990, **9**, 142.
86. J. Farkas, K. M. Chi, M. J. Hampden-Smith, T. T. Kodas and L. Dubois, *J. Appl. Phys.* 1993, **73**, 1455.
87. M. J. Hampden-Smith and T. T. Kodas, *Mater. Res. Soc. Bull.* 1993, **XVIII**, 39.
88. F. Rousseau, J. Jain, T. T. Kodas, M. J. Hampden-Smith, J. D. Farr and R. Muenchausen, *J. Mater. Chem.* 1992, **2**, 893.
89. C. Roger, T. S. Corbitt, M. J. Hampden-Smith and T. T. Kodas, *Appl. Phys. Lett.* 1993, **65**, 1021.
90. C. Y. Xu, M. J. Hampden-Smith and T. T. Kodas, *Angew. Chem. Adv. Mater.* 1994, **6**, 745.
91. B. N. Hansen, B. M. Hybertson, R. M. Barkley and R. E. Sievers, *Chem. Mater.* 1992, **4**, 749.
92. H. H. Gysling and A. A. Wernberg, *Chem. Mater.* 1992, **4**, 900.
93. R. D. Pike, H. Cui, R. Kershaw, K. Dwight, A. Wold, T. N. Blanton, A. A. Wernberg and H. J. Gysling, *Thin Solid Films* 1993, **224**, 221.
94. A. A. Wernberg and H. J. Gysling, *Chem. Mater.* 1993, **5**, 1056.
95. G. Blandenet, M. Court and Y. Legard *Thin Solid Films* 1981, **77**, 81.
96. C. Xu, M. J. Hampden-Smith, T. T. Kodas, E. N. Duesler, *J. Chem. Soc., Dalton Trans.* 1994, 2841.
97. A. Bailey, T. S. Corbitt, M. J. Hampden-Smith, E. N. Duesler and T. T. Kodas, *Polyhedron* 1993, **12**, 1785.
98. A. Jain, K.-M. Chi, H. K. Shin, M. J. Hampden-Smith, T. T. Kodas, M. F. Paffett and J. D. Farr, in *SPIE Conf. Proc.*, Vol. 1596, pp. 23. San Jose, CA (1991).